Org Divers Evol (2017) 17:267–285
DOI 10.1007/s13127-016-0293-3

ORIGINAL ARTICLE

ORGANISMS DIVERSITY & EVOLUTION

Endemic diversification in the mountains: genetic, morphological, and geographical differentiation of the *Hemidactylus* geckos in southwestern Arabia

Jiří Šmíd[1,6] · **Mohammed Shobrak**[2] · **Thomas Wilms**[3] · **Ulrich Joger**[4] · **Salvador Carranza**[5]

Received: 18 January 2016 / Revised: 8 June 2016 / Accepted: 30 June 2016 / Published online: 12 July 2016

Abstract In this study, we provide genetic, morphological, and geographical comparisons for 11 species of the southwestern Arabian radiation of *Hemidactylus* geckos, nine of which are endemic to the region. By using a coalescence-based species-tree reconstruction in combination with divergence time estimations and speciation probability testing, we show that most of the speciation events occurred in the Pliocene, which is more recent than previously thought based on calibrations of concatenated data sets. The current dating indicates that the changing climate at the beginning of the Pliocene, from hot and dry to cold and wet, is likely responsible for increased speciation in *Hemidactylus*. Analyses of geographic and altitudinal overlap of the species and their morphological differentiation show that most species do not occur in sympatry. Those that overlap geographically are usually differentiated by their altitudinal preference, head shape, body size, or their combination. Our results indicate that the topographically complex mountains of southwestern Arabia support a significant radiation of *Hemidactylus* geckos by allowing multiple allopatric speciation events to occur in a relatively small area. Consequently, we describe two new species endemic to the Asir Mountains of Saudi Arabia, *H. alfarraji* sp. n. and *H. asirensis* sp. n., and elevate two former subspecies of *H. yerburii* to a species level, *H. montanus* and *H. pauciporosus*.

Keywords Allopatry · Diversity · Gekkonidae · Radiation · Species delimitation · Species tree · Speciation

Electronic supplementary material The online version of this article (doi:10.1007/s13127-016-0293-3) contains supplementary material, which is available to authorized users.

✉ Jiří Šmíd
jirismd@gmail.com

[1] Department of Zoology, National Museum, Cirkusová 1740, Prague, Czech Republic

[2] Biology Department, Faculty of Science, Taif University 888, Taif, Saudi Arabia

[3] Allwetterzoo Münster, Sentruper Straße 315, 48161 Münster, Germany

[4] Staatliches Naturhistorisches Museum Braunschweig, Gaußstraße 22, 38106 Braunschweig, Germany

[5] Institute of Evolutionary Biology (CSIC-Universitat Pompeu Fabra), Passeig Marítim de la Barceloneta 37-49, Barcelona, Spain

[6] South African National Biodiversity Institute, Private Bag X7, Claremont, Cape Town, South Africa

Introduction

Montane areas have been traditionally viewed as bleak environments impoverished in terms of biodiversity, especially when compared to lowland areas of the same region (Fjeldså et al. 2012). However, recent studies show that montane areas act as significant reservoirs of species richness that stand out from the intervening lowlands not only topographically, but also biologically (e.g., McCormack et al. 2009; Kohler and Maselli 2012). This is particularly true for tropical and subtropical mountains that have not been severely affected by glacial climatic oscillations (e.g., Fjeldså and Rahbek 2006; Popp et al. 2008; Wollenberg et al. 2008; Pepper et al. 2011). They are also recognized as areas of high priority for conservation, primarily due to substantial numbers of endemic species with narrow distribution ranges easily threatened by extinction (Myers et al. 2000; Mittermeier et al. 2004).

While most of the Arabian Peninsula is flat and covered by vast and harsh deserts, the mountain ranges rimming it from the west and south constitute prominent topographic features

that protrude from the surrounding plateaus, in particular, the Asir Mountains of Yemen and Saudi Arabia, towering up to over 3000 m, rising from the Tihamah Desert. They form a broad plateau and, with their rugged topography (Fig. 1), represent structurally complex habitats and landscape types. The high elevation of the main ridge and the sharp escarpment influence the climate in the area significantly. The annual precipitation in the mountains is as much as six times higher than in the adjoining lowlands, being a result of the seasonal southwestern monsoon (also known as Khareef) that drenches the mountains from June until September (Edgell 2006).

The initial uplift of the mountain ranges began with the opening of the Red Sea in the Oligocene some 30 million years ago (Ma) (Bosworth et al. 2005). The mountains rose further and tilted up to the east during the Miocene (~15 Ma) as a result of Arabia's rifting and volcanism (Bohannon et al. 1989; Davison et al. 1994). The geological evolution of Arabia has also affected the climate of the region. The climate fluctuated in cycles from extremely hot and hyper arid at the beginning of the Miocene to wetter and temperate semi-arid conditions during the Pliocene, and back to arid conditions in the Quaternary (Edgell 2006; Huang et al. 2007).

The uniqueness of Southwestern (SW) Arabia's mountain ranges and its climate is further reflected by the high proportion of endemic species present. It has the richest reptile diversity in Arabia (Cox et al. 2012), with 102 species, subspecies, and putative species yet to be described of terrestrial reptiles currently known to occur in SW Arabia (Sindaco and Jeremčenko 2008; Sindaco et al. 2013; work in progress). Of these, 42 taxa (41 %) are endemic. Geckos (Gekkota) are represented by eight genera (*Bunopus*, *Cyrtopodion*, *Hemidactylus*, *Stenodactylus*, *Tropiocolotes, Ptyodactylus, Pristurus, Trachydactylus*), with 26 species representing a substantial portion of the herpetofauna of this Arabian hotspot area. The genus *Hemidactylus* is the most species-rich of all reptile genera in the area, with ten recognized species and subspecies. Having undergone numerous taxonomic adjustments within recent years, it is by far the best studied reptile genus on the Arabian peninsula (Busais and Joger 2011a, b; Moravec et al. 2011; Carranza and Arnold 2012; Gómez-Díaz

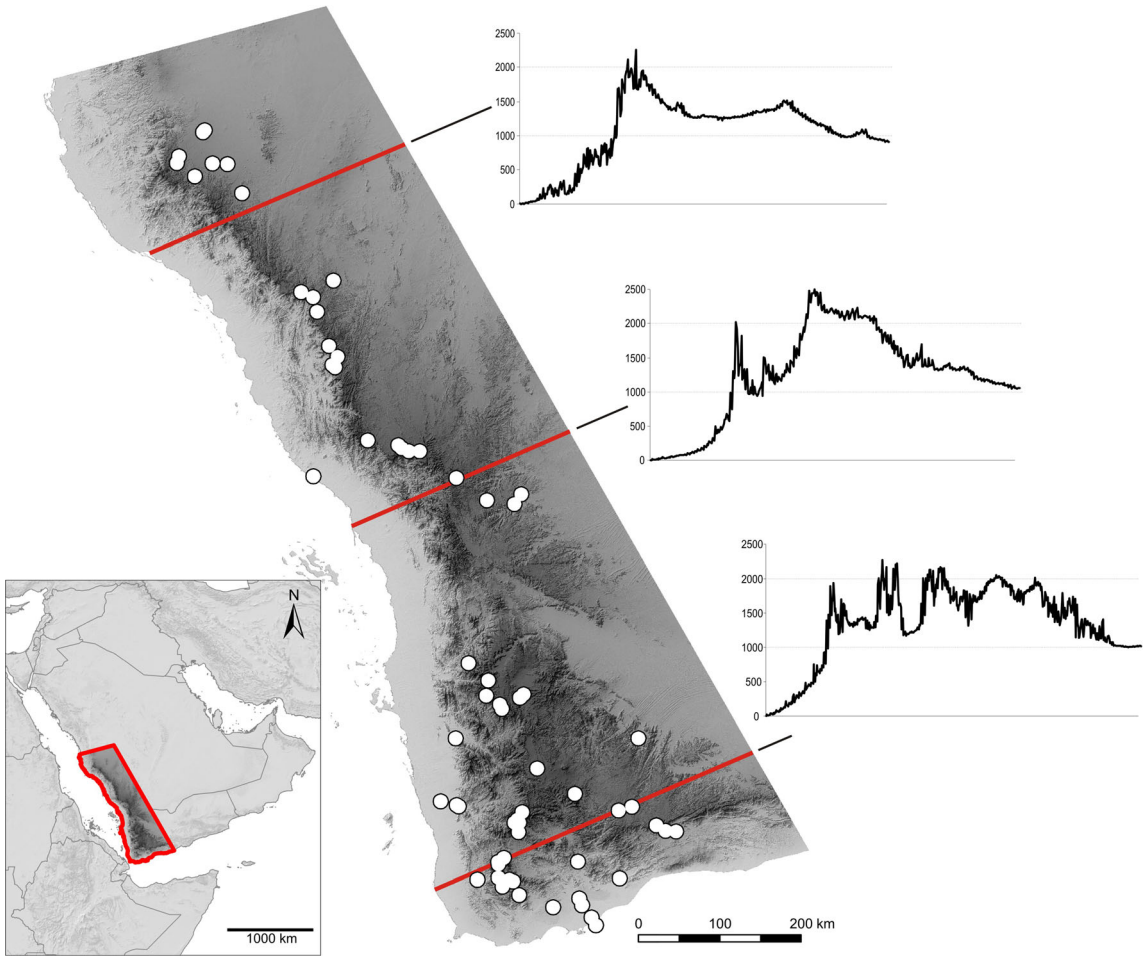

Fig. 1 The extent of the study encompassing the highlands of Yemen and the Asir Mountains of Saudi Arabia and showing sampling localities from which material for genetic analyses was used. Elevation profiles at three sections that show the topography of the region are indicated by the *red lines*. (Color figure online)

et al. 2012; Šmíd et al. 2013a, b, 2015; Vasconcelos and Carranza 2014). Nine of the ten taxa are part of the Arid clade of *Hemidactylus* (Carranza and Arnold 2006), which underwent major radiation in Arabia subsequent to Arabia's separation from the African landmass (Šmíd et al. 2013a). Of the nine, seven are endemic to SW Arabia (*H. adensis* Šmíd et al. 2015; *H. jumailiae* Busais and Joger, 2011; *H. mandebensis* Šmíd et al. 2015; *H. saba* Busais and Joger, 2011; *H. ulii* Šmíd et al., 2013; *H. yerburii yerburii* Anderson 1895; *H. y. montanus* Busais and Joger, 2011), *H. granosus* Heyden, 1827 extends in range to the Sinai Peninsula, and *H. robustus* Heyden, 1827 is believed to have been introduced by humans. These species form two monophyletic groups that are not closely related (Šmíd et al. 2013a). One is sister to an African group and the other has an African species nested within it (*H. awashensis* Šmíd et al. 2015). All these African species originated in southern Arabia, and the dating estimates suggest that the colonization of Africa occurred in the Late Miocene (Šmíd et al. 2013a), which emphasizes the dispersal ability of geckos and underscores the close biogeographic connection between Africa and Arabia.

In this study, we provide novel data on the phylogeny of all species within the Arid clade of *Hemidactylus* from SW Arabia. We reconstruct the phylogeny using a coalescent-based species-tree estimation and simultaneously estimate the divergence times to compare the results with previously published dates based on concatenated analyses. The probability of speciation at each node of our phylogeny is tested in order to assess the species limits and the credibility of the current taxonomy of *Hemidactylus*. As a result, we describe two new species endemic to the mountains of Saudi Arabia and elevate two subspecies to species level. Finally, we test the geographical and altitudinal differentiation, as well as the morphological niche partitioning in this major endemic radiation of *Hemidactylus* from SW Arabia.

Materials and methods

Study area

The extent of this study was selected to encompass the major mountain ranges of SW Arabia—the Yemeni highlands and the Asir Mountains of Saudi Arabia adjoining to the north. It forms a strip approximately 400 km in width spanning from the southwestern corner of the peninsula to Jeddah (roughly 22° of latitude) in the north (Fig. 1).

Material for phylogenetic analyses

New material (67 samples and voucher specimens) was collected during a field trip to Saudi Arabia in May–June 2012. Additional tissue samples were obtained from collections listed in Table S1. A total of 108 new samples were combined with sequences of all species from the Arabian and Socotran radiations of *Hemidactylus*, which resulted in a data set of 339 samples.

DNA extraction and sequencing

For the new material and museum samples, genomic DNA was extracted using commercially available kits. Concordantly with our previous phylogenetic studies on *Hemidactylus* (Carranza and Arnold 2012; Šmíd et al. 2013a, b, 2015), we PCR-amplified and sequenced the following genes: 12S ribosomal RNA (*12S*—ca. 425 bp) and cytochrome *b* (*cytb*—1137 or 307 bp, depending on the amplification success and primers) from the mitochondrial DNA (mtDNA) and the proto-oncogene mos (*cmos*—402 bp), the melanocortin 1 receptor (*mc1r*—666 bp), and the recombination activating genes 1 and 2 (*rag1*—1024 bp, *rag2*—408 bp) from the nuclear DNA (nDNA). Primer sequences and PCR conditions are given elsewhere (Šmíd et al. 2013a). Both the forward and reverse strands were sequenced. Chromatograms were checked by eye, and contigs were assembled and edited in Geneious v.6 (Biomatters Ltd.). All genes were aligned independently in MAFFT v.7 (Katoh and Standley 2013) using the Q-INS-i settings for the *12S* alignment and the "auto" settings for all other genes. Regions of the *12S* alignment containing many indels were removed with Gblocks (Castresana 2000) with the less stringent selection applied (Talavera and Castresana 2007), which resulted in an alignment of 380 bp. All protein-coding genes were translated to amino acids, and no stop codons were detected.

Sample details including collection codes, countries of origin, localities, GPS coordinates, and corresponding GenBank accession numbers are presented in Table S2. Details on the origin and GenBank accessions of the other Arid clade species included in the maximum likelihood analysis (see below) that do not belong to the target groups can be found elsewhere (Šmíd et al. 2013a).

Phylogenetic analyses

Maximum likelihood of mtDNA data

To reconstruct the phylogenetic relationships of the SW Arabian *Hemidactylus*, we performed several independent analyses on two data sets. To infer the position of the newly acquired material within the Arabian radiation, we used all the 339 samples and the two mtDNA genes concatenated (1517 bp, data set 1). The best-fit model of nucleotide evolution of this data set was identified by PartitionFinder (Lanfear et al. 2012) under the following

settings: greedy search, branch lengths linked, only models available in RAxML evaluated, and BIC selection criterion applied. The best scheme preferred four independent partitions: *12S*, *cytb* position1, *cytb* position2, and *cytb* position3, with GTR+I+G model suggested for all. A maximum likelihood (ML) phylogenetic analysis of data set 1 was conducted in RAxML v.7.3 (Stamatakis 2006) using raxmlGUI v.1.2 interface (Silvestro and Michalak 2012). Heuristic search included 100 random addition replicates with parameters estimated independently for each partition and with 100 thorough bootstrap pseudoreplications. The GTRGAMMA model was used for all partitions as recommended over the GTRGAMMAI in the program manual. Identical haplotypes were excluded from the analysis. Eight individuals representing four species of the Socotran radiation, which is sister to the Arabian radiation of the genus (Gómez-Díaz et al. 2012; Šmíd et al. 2013a), were used to root the tree (*H. dracaenacolus*—IBES 2604, IBES 3922, IBES 3940; *H. granti*—IBES 5307, IBES 5626; *H. inintellectus*—IBES 5068; *H. pumilio*—IBES 5021, IBES 5117). By using ML analysis, we identified the monophyletic groups in which all the SW Arabian species of the *Hemidactylus* Arid clade belong—the *saba* group (consisting of *H. saba*, *H. granosus*, *H. ulii*, and the two new species described herein), the *robustus* group (*H. robustus*, *H. adensis*, *H. awashensis*, *H. mandebensis*) as termed in previous studies (Šmíd et al. 2013b, 2015), and the *yerburii* group defined here for the first time (*H. yerburii yerburii*, *H. yerburii montanus*, *H. yerburii pauciporosus*, *H. barodanus*, *H. granchii*, *H. jumailiae*, *H. macropholis*).

Intraspecific and interspecific uncorrected pairwise distances (*p* distances) of the *12S* and *cytb* gene fragments were calculated in MEGA6 (Tamura et al. 2013) using the pairwise deletion options.

Haplotype networks

Genealogical relationships within the three groups of *Hemidactylus* in the four analyzed nuclear markers were assessed with haplotype networks. Heterozygous positions were identified based on the presence of two peaks of approximately equal height at a single nucleotide site in both strands (assessed by eye and Heterozygote Plugin as implemented in Geneious) and were coded using IUPAC ambiguity codes. Haplotypes were inferred using PHASE v.2.1 (Stephens et al. 2001) with the probability threshold set to 0.7. SeqPHASE (Flot 2010) was employed to convert the input and output files. Since the presence of distant taxa in the alignment can strongly affect the results of phasing, the *yerburii* group was phased and independent networks were produced for it separately from the *saba* and *robustus* groups, which were phased together since they are closely related. Because it has been shown that the presence of missing data can result in misleading networks (Joly et al. 2007), samples with sequences much shorter than the rest of the alignment were removed and the alignment was trimmed to the length of the shortest sequence. The trimmed alignments had the following lengths: *cmos* 363 bp and *rag1* 941 bp for the *yerburii* group; *rag1* 870 bp and *mc1r* 661 bp for *saba* and *robustus* groups; otherwise, the length was identical to the original (see above). Haplotype networks were constructed with TCS v.1.21 (Clement et al. 2000) using statistical parsimony with 95 % connection limit (Templeton et al. 1992) and were visualized with tcsBU (dos Santos et al. 2015).

Species tree

To reliably estimate the divergence times of the studied *Hemidactylus* groups (*yerburii*, *robustus*, *saba*), we combined all 16 species forming these groups in one data set (3924 bp, data set 2) and performed a multigene coalescent-based species tree estimation in *BEAST (Heled and Drummond 2010). The analysis was performed in BEAST v.1.8 (Drummond et al. 2012). In total, 124 specimens were used in this analysis (Table S2). The number of gene copies per species ranged from 2 to 36 across all genes with the only exception being *rag1*, which failed to amplify for *H. y. pauciporosus*. "Species" need to be defined prior to the species tree analysis, but since the taxonomy of the Arabian *Hemidactylus* is very advanced, we used species and subspecies as defined in previous studies. The only exception were 14 samples from Saudi Arabia that formed two isolated clusters within the *saba* group as reconstructed by the ML analysis and that were also considered as two independent "species" for the species tree estimation. The probability of their speciation was further tested (see below). Because the Bayesian time-tree analysis in BEAST samples the root position from the posterior along with the rest of the tree topology (Drummond and Bouckaert 2015), we did not use any a priori outgroup to root the tree. Nuclear markers were imported into BEAUTI after being phased (see above). Since the species tree estimation assumes no recombination within loci, we tested all four nDNA genes for traces of recombination using the RDP, GENECONV, and MaxChi methods in RDP v.4 (Martin et al. 2010) and no recombination was detected. Best-fit substitution models for each gene were identified by AIC selection criterion as implemented in jModelTest v.2.1 (Darriba et al. 2012): *12S* and *cytb*—GTR+I+G, *cmos* and *rag1*—HKY+I, *mc1r* and *rag2*—HKY+I+G. Substitution, clock, and tree models were unlinked across all partitions. Base frequencies were set to empirical and the ploidy type of the two mtDNA genes to mitochondrial. We used a likelihood ratio test (LRT) implemented in MEGA6 to test if the genes studied evolve in a clock-like manner. The clock-like evolution of all genes was rejected at a 5 % significance level; a relaxed uncorrelated

lognormal clock prior was therefore selected for all of them. Other prior settings were as follows (otherwise by default): Yule process tree prior with birth rate uniform (lower 0, upper 1000), random starting trees, GTR base substitution prior uniform (0, 100), alpha prior uniform (0, 10), and proportion of invariable sites uniform (0, 1). The nDNA alignments still contained some unresolved heterozygous positions after being phased. In order to account for variability in these heterozygous positions, we removed the operator on kappa (HKY transition-transversion parameter), gave it an initial value of 0.5, and modified manually the xml file by changing the "useAmbiguities" parameter to "true." Three individual runs were performed each of 5×10^8 generations with parameters logged every 5×10^4 generations. Posterior trace plots, stationarity, convergence, and effective sample size (ESS) of the parameters were inspected in Tracer v.1.5 (Rambaut and Drummond 2007). The tree files resulting from the three runs were combined using LogCombiner v.1.7 discarding 10 % of each run as burn-in, and a maximum clade credibility (MCC) tree was produced from the 27,000 sampled trees using TreeAnnotator v.1.7 (both programs are part of the BEAST package). Nodes with posterior probability (pp) values ≥0.95 were considered strongly supported. Original concatenated alignments of data sets 1 and 2 in FASTA format and Geneious annotated format (compatible with version 6.0 and later) together with the resulting phylogenetic trees (NEWICK format) are available at MorphoBank under Project 2227 (http://www.morphobank.org/).

Estimation of divergence times

The complete absence of any *Hemidactylus* fossil record found in literature (Estes 1983) or in public databases such as Fossilworks (http://fossilworks.org/) or fosFARbase (Böhme and Ilg 2003) that could be used as internal calibration point precludes direct estimation of the time of the speciation events in our phylogeny. We, therefore, used a prior on the global substitution rates of the same *12S* and *cytb* regions calculated from a comprehensive phylogenetic study of several squamate groups (Carranza and Arnold 2012). These rates have been corroborated by independent studies of different taxa that used different calibration points (Metallinou et al. 2012; Sindaco et al. 2012). Specifically, we set a lognormal prior distribution on the ucld.mean parameters of the *12S* and *cytb* partitions with mean value = 0.00755 for the *12S* and 0.0228 for the *cytb* and a normal prior distribution on the ucld.stdev with mean value = 0.00247 for the *12S* and 0.00806 for the *cytb*. The estimated ucld.mean and ucld.stdev parameters for the nDNA genes were set to have a lognormal prior distribution with initial value = 0.001, mean = 0, and stdev = 1 and exponential prior distribution with initial value = 0.001 and mean = 0.001, respectively.

Topology test

All three currently recognized subspecies of *H. yerburii* are part of the same species group as revealed by the ML analysis of data set 1, yet they do not cluster into a monophyletic group (Fig. S1). Although *Hemidactylus y. yerburii* is sister to *H. y. montanus*, *H. y. pauciporosus* forms a well-supported clade with the other African species (*H. barodanus*, H. *granchii*, *H. macropholis*). We tested for monophyly of all *H. yerburii* subspecies by means of Bayes factor (BF) that compares relative support of competing hypotheses given the input data (Kass and Raftery 1995). For the computational demands required to estimate the marginal likelihood, we confined the analysis to the *yerburii* group only. We first generated a species tree without any topological constraints using the full set of genes and settings as described above. Concurrently, we generated a species tree with the alternative topology in which monophyly of *H. y. yerburii*, *H. y. montanus*, and *H. y. pauciporosus* was constrained. Marginal likelihood (log) for each topology was estimated using path sampling (PS) and stepping-stone sampling (SS) (Baele et al. 2012, 2013) as implemented in BEAST v.1.8, which have been shown to work well within a multi-species coalescent framework and to outperform other estimators (Grummer et al. 2014), and BF was calculated as the difference of log marginal likelihoods of the unconstrained and constrained trees. The analyses were run on the CIPRES Science Gateway (Miller et al. 2010).

Speciation probabilities

To test the probability of speciation at each node of our phylogeny, we used a Bayesian modeling approach implemented in Bayesian Phylogenetics and Phylogeography (BPP v.3) (Rannala and Yang 2003; Yang and Rannala 2010). The method requires a fully resolved tree as a guide tree from which subtrees are generated by collapsing or splitting nodes. Reversible-jump Markov chain Monte Carlo (rjMCMC) algorithm then estimates the posterior distribution for species delimitation models and provides a speciation probability for each node (Leaché and Fujita 2010). BPP has been shown to perform well even with a relatively small number of loci (Camargo et al. 2012).

Two groups were analyzed independently: (1) the *yerburii* group and (2) the closely related *saba* and *robustus* groups. The guide tree topology was specified using the relationships inferred by *BEAST. We analyzed two types of data—all markers (two mtDNA + four nDNA phased) combined and the nDNA (phased) alone. We ran the rjMCMC analyses for 10^5 generations with 20 % samples discarded as burn-in. Following the suggestions of Leaché and Fujita (2010), we analyzed three combinations of priors for the ancestral population size (θ) and root age (τ) with a gamma distribution G(α,

β): (1) a relatively large ancestral population size and deep divergences among species (θ = G(1, 10) and τ = G(1, 10)); (2) a relatively small ancestral population size and shallow divergences among species (θ = G(2, 2000) and τ = G(2, 2000)); and (3) a relatively large ancestral population size with shallow divergences among species (θ = G(1, 10) and τ = G(2, 2000)). Each analysis was conducted twice, using reversible-jump algorithm 0 (with parameter $\varepsilon = 2$) and algorithm 1 (with parameters $\alpha = 2$ and m = 1), respectively (Yang and Rannala 2010). The heredity parameter that allows θ to vary among loci was estimated with a gamma prior G(4, 4), and the locus rate parameter that allows variable mutation rates among loci was estimated with a Dirichlet prior ($\alpha = 2$). The optimal acceptance proportions were controlled to fall in the interval (0.15, 0.7) suggested by Yang (2014). Speciation at nodes with speciation probability values ≥0.95 was interpreted as strongly supported (Leaché and Fujita 2010).

Geographic and altitudinal overlap

For the paucity of direct field evidence of sympatry/allopatry in SW Arabian *Hemidactylus*, we used geographic overlap of species ranges as a surrogate for this measure. For each species, the range was estimated by drawing a convex polygon around all available localities within the extent of the study (for a complete list of localities, see Table S2) with the convex hull function of XTools Pro v.11.1 extension for ArcGIS v.10 with the hull detail level set to 50. Additionally, a 10-km buffer was added to each hull to account for the uncertainty associated with the estimate of geographic coordinates of museum specimens. The exceptions were *H. granosus*, which is known to occur also outside the extent used here and for which all known records were used; *H. robustus*, which is known to be distributed only along the coasts being most likely a result of having been introduced there by man and for which the polygon was drawn by hand as a 50–100-km-wide belt along the coast; and *H. saba*, which has so far only been recorded from one locality and for which only the 10-km buffer was drawn. We consider two species to live in sympatry if at least 10 % of the range of one of them lies within the range of the other.

To determine pairwise significance of species altitudinal diversification, we used one-way ANOVA with unequal sample size honest significant difference (HSD) post hoc test performed in Statistica v.8 (StatSoft Ltd.). For *H. granosus* distributed also outside the extent of this study, we used all available altitudinal data because the species has very shallow population structuring and local adaptation is thus unlikely, while for *H. robustus* that has a vast range spanning from Kenya to Egypt in the northwest and India in the northeast, adaptation to local conditions is more plausible, especially given its higher intraspecific genetic diversification, and we therefore used altitude data only from within the extent of this study. Altitude data are given in Table S2.

Material for morphological analyses

Morphological analyses were performed on 247 individuals. The number of individuals ranged from 3 (*H. mandebensis*, *H. saba*, all specimens ever reported for both species) to 94 (*H. y. montanus*). It is of paramount importance for the taxonomic outcomes of this study that of the 11 SW Arabian species (9 recognized + 2 described herein), name-bearing type specimens were examined for nine of them and high-quality photographs were available for all of them. Apart from that, additional 68 paratype specimens and one paralectotype were examined and included in the analyses. The African species were excluded from the morphological analyses. Only *H. y. pauciporosus* measurements were used for a comparison with *H. y. yerburii* and *H. y. montanus*. The list of specimens examined morphologically including the original morphological data is shown in Table S2; the list of collection acronyms from where material was obtained is shown in Table S1. High-resolution original photographs of 214 vouchered specimens (totaling in 2891 pictures) of *H. jumailiae*, *H. y. yerburii*, *H. y. montanus*, *H. y. pauciporosus*, and the two new species described herein were deposited and are available at MorphoBank. Photographs of most of the other species can be found at the same repository under the following project numbers: Project 1006 (*H. granosus*, *H. saba*, *H. ulii*; Šmíd et al. 2013b), Project1069 (*H. granchii*; Šmíd et al. 2014), and Project1172 (*H. adensis*, *H. awashensis*, *H. mandebensis*, *H. robustus*; Šmíd et al. 2015).

Morphological analyses

We took the following metric and meristic measurements using a digital caliper (rounding to 0.1 mm): snout-vent length (SVL), tail length (TL), head length (HL), head width (HW), head depth (HD), left eye diameter (E), axilla-groin distance (AG), number of infralabials (INF) and supralabials (SUP); contact of uppermost nasals (NASCON); number of infralabials in contact with anterior postmentals (MENINF); mutual position of anterior postmentals (MENCON); number of longitudinal rows of enlarged dorsal tubercles (TUBER); number of lamellae under the first (1TOE) and fourth (4TOE) toe of hind legs; and number of preanal pores in males (PORES). The characters were measured as described in detail elsewhere (Šmíd et al. 2015).

To test for the morphological differentiation, we compared features that are often associated with interspecific disparity in lizards and that reflect the species ecological niche, such as prey size or habitat use—body size (represented by SVL) and head shape (e.g., Vanhooydonck and Van Damme 1999; Herrel et al. 2001; Losos 2009). Head shape was quantified

by means of a principal component analysis (PCA, performed in Statistica) of the HL, HD, HW, and E variables. The effect of body size on the head variables was removed by regressing them (log_{10}-transformed) against log_{10}-transformed SVL and using the residuals as PCA input data. The number of significant components was determined by the broken-stick model (Frontier 1976). These components were further tested by unequal n HSD post hoc test of factorial MANOVA to determine the significance of between-species differences. Body size differences between species were tested by one-way ANOVA unequal n HSD post hoc test with original, untransformed SVL data used as input. Because sexual dimorphism is absent in the Arid clade of *Hemidactylus* in the original metric values (Carranza and Arnold 2012) as well as in the size-corrected head proportions (Student's *t* test corrected for multiple comparisons with a Bonferroni correction; data not shown), we analyzed both sexes together. Meristic characters and body size variables not employed in the PCA were used for interspecific comparisons.

Results

Phylogenetic analyses

The ML analysis of the mtDNA data for the 339 individuals which represented 259 unique haplotypes resulted in the tree shown in Fig. S1. All Arid clade *Hemidactylus* species that occur within the extent of this study fall within three well-supported groups: (1) the *yerburii* group (bootstrap support 93) formed by *H. y. yerburii*, *H. y. montanus*, *H. jumailiae*, and four other species and subspecies from the adjoining Africa (*H. y. pauciporosus*, *H. barodanus*, *H. granchii*, *H. macropholis*); (2) the *robustus* group (bootstrap 100) formed by *H. robustus*, *H. adensis*, *H. awashensis*, and *H. mandebensis*; and (3) the *saba* group (bootstrap 95) formed by *H. saba*, *H. ulii*, *H. granosus*, and two new species described herein. Mean genetic distances of the mtDNA genes (*12S* and *cytb*) between all these taxa are given in Table S3.

In most genes, there is a certain degree of allele sharing between species in both the *yerburii* group and the *robustus* + *saba* groups with the only exception of the *mc1r* network of the *yerburii* group, in which all species are clearly separated and do not share a single allele (Fig. 2b). On the other hand, networks of *cmos* and *rag2* of both groups and *mc1r* of the *robustus* + *saba* group show allele sharing between all sister species. Within the *yerburii* group, all markers support the close relationship of *H. y. yerburii* and *H. y. montanus*.

All three independent runs of the *BEAST analysis converged with ESS values >200, a critical value recommended in the BEAST manual indicating adequate mixing of the MCMC analyses. The *BEAST results are shown in Fig. 2a. *Hemidactylus awashensis* was identified as a sister taxon to all the other species of the *robustus* group, and the three remaining species were supported to form a clade (pp = 0.97). In the *saba* group, the position of *H. granosus* as sister to the new species endemic to the Asir Mountains described herein was supported (pp = 1.0), as well as the sister relationship of the clade of these two as sister to the new species from Najran also described herein (pp = 1.0). Otherwise, the deeper phylogenetic relationships within this group were not supported. Within the *yerburii* group, *H. y. yerburii* and *H. y. montanus* were highly supported as sister taxa (pp = 1.0), closely related to *H. jumailiae* (pp = 1.0).

Estimation of divergence times

The basal split within the *yerburii* group took place 6.6 Ma (95 % highest posterior density interval (HPD) 5.4–7.9), the basal split in the *robustus* group 4.2 Ma (HPD 3.3–5.1), and that in the *saba* group 5.6 Ma (HPD 4.6–6.6) (Fig. 2a). The split between *H. y. yerburii* and *H. y. montanus* was dated back to 1.7 Ma (HPD 1.0–2.5). The split of *H. granosus* from one of the new species described herein occurred relatively recently, 0.9 Ma (HPD 0.4–1.3). These two separated from the other new species described herein 2.8 Ma (HPD 1.8–3.9).

Topology test

The results of the topology test for which the three *H. yerburii* subspecies (*H. y. yerburii*, *H. y. montanus*, *H. y. pauciporosus*) were forced to form a monophyletic group and tested against our optimal topology from Fig. 2a by means of Bayes factor indicate that our optimal topology was strongly favored and that *H. y. pauciporosus* was decisively excluded from this clade (log BF >25 in both PS and SS sampling marginal likelihood estimations) following the classification by Kass and Raftery (1995).

Speciation probabilities

Bayesian species delimitation supported with high speciation probabilities (≥0.95) that all the species analyzed underwent a speciation event (Fig. 2a). The sole exception was the sister species pair *H. granchii–H. y. pauciporosus* that under a large ancestral population size prior (θ = G(1, 10)) received low support of the speciation event regardless of root age prior and the algorithm employed (BPP pp = 0.81 for τ = G(1, 10); BPP pp = 0.83 for τ = G(2, 2000)). Otherwise, all combinations of prior settings, input data types (mtDNA + nDNA vs. nDNA alone), and algorithm used supported speciation events in all nodes of the tree. It has been shown that the inclusion of mtDNA in the Bayesian species delimitation analyses can influence the results (Burbrink and Guiher 2015); therefore, we only show and interpret the BPP results of the analyses of the four nuclear genes.

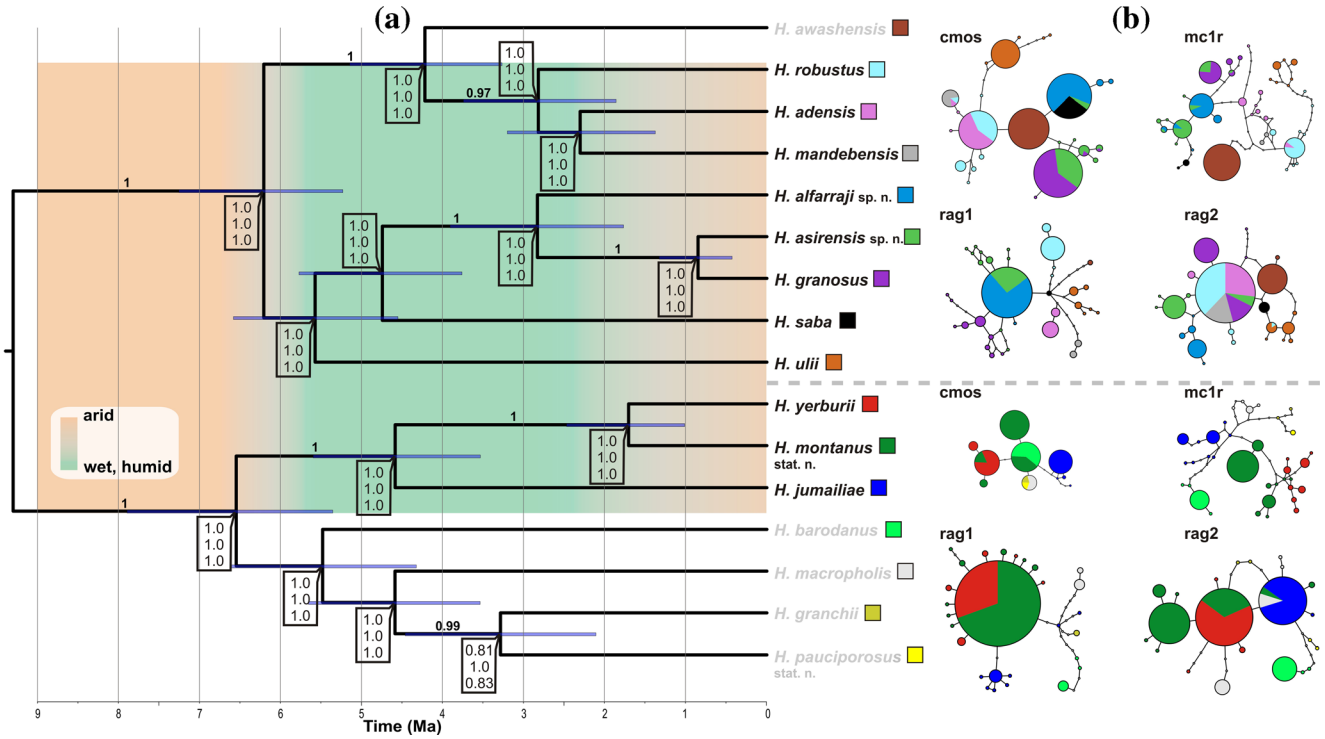

Fig. 2 **a** Maximum clade credibility (MCC) tree of the *robustus*, *saba*, and *yerburii* groups of the Arabian *Hemidactylus* resulting from the *BEAST analysis and inferred using two mtDNA and four nDNA gene fragments. Posterior probability values ≥0.95 are shown above branches. The *tree* is a time tree, the *scale* at the bottom indicates the age estimates of the speciation events in millions of years (Ma), and the *blue bars* indicate 95 % HPD intervals. *Numbers in square boxes* show speciation probabilities for each node as inferred by BPP based on the nDNA data set under the following combinations of ancestral population size and root age priors (*top* to *bottom*): large ancestral population and deep divergences among species, small ancestral population and shallow divergences among species, and large ancestral population and shallow divergences among species. African species that do not occur within the extent of this study but are closely related to the Arabian species dealt with herein are in *grey*. The *background coloration* indicates changes in historical climatic conditions in Arabia from extremely hot and arid in the Miocene to wetter and humid throughout most of the Pliocene and then back to hyper arid in the Quaternary. **b** Nuclear allele networks of the four analyzed nuclear loci. *Circle sizes* are proportional to the number of alleles. *Small empty circles* represent mutational steps. *Colors* correspond to those given after species names. The *dashed line* separates the two data sets for which networks were drawn independently. (Color figure online)

Geographic and altitudinal overlap

Ranges of all species estimated by the convex hull and 10-km buffer functions are presented in Fig. 3. The estimated ranges of the endemic species cover from over 300 km^2 in *H. saba* to 79,000 km^2 in *H. y. montanus*. Out of the 55 available pairwise comparisons between the 11 SW Arabian species, only 15 were found to overlap in more than 10 % of ranges and were therefore considered sympatric under our criteria (Fig. 4). On the contrary, only 16 species pairs were identified to be significantly different in their altitudinal preferences by HSD post hoc test ($p < 0.05$) (Fig. 4).

Morphological analyses

The first three PCA components were identified as significant by the broken-stick model. Combined, they accounted for 91.9 % of the variability (PC1 54.9 %, PC2 21.4 %, PC3 15.6 %). The first component mostly corresponded to residuals of head width, the second to residuals of head depth, and the third to residuals of eye diameter (all $\log_{10}$-transformed against $\log_{10}$ SVL). The PC1 and PC2 axes show the species cloud clearly stretched along the narrow-flat (relative to body size; lower left corner) to broad-high head (relative to body size; upper right corner) continuum (Fig. S2). Fifteen species pairs were identified as significantly different in head shape while 20 species pairs differed significantly in body size (SVL) by HSD post hoc test (Fig. 4).

Taxonomic implications

Several taxonomic implications for the genus *Hemidactylus* stem from our analyses. The three subspecies of *H. yerburii* were not recovered as monophyletic in the *BEAST analysis with *H. y. pauciporosus* being nested within the other African species of this clade and sister to *H. granchii*, from which it separated 3.3 Ma (HPD 2.1–4.5; Fig. 2a). It also does not share any allele with either of the two other subspecies (Fig. 2b). Most of all, the alternative topology in which the three subspecies were forced to form a monophyletic group

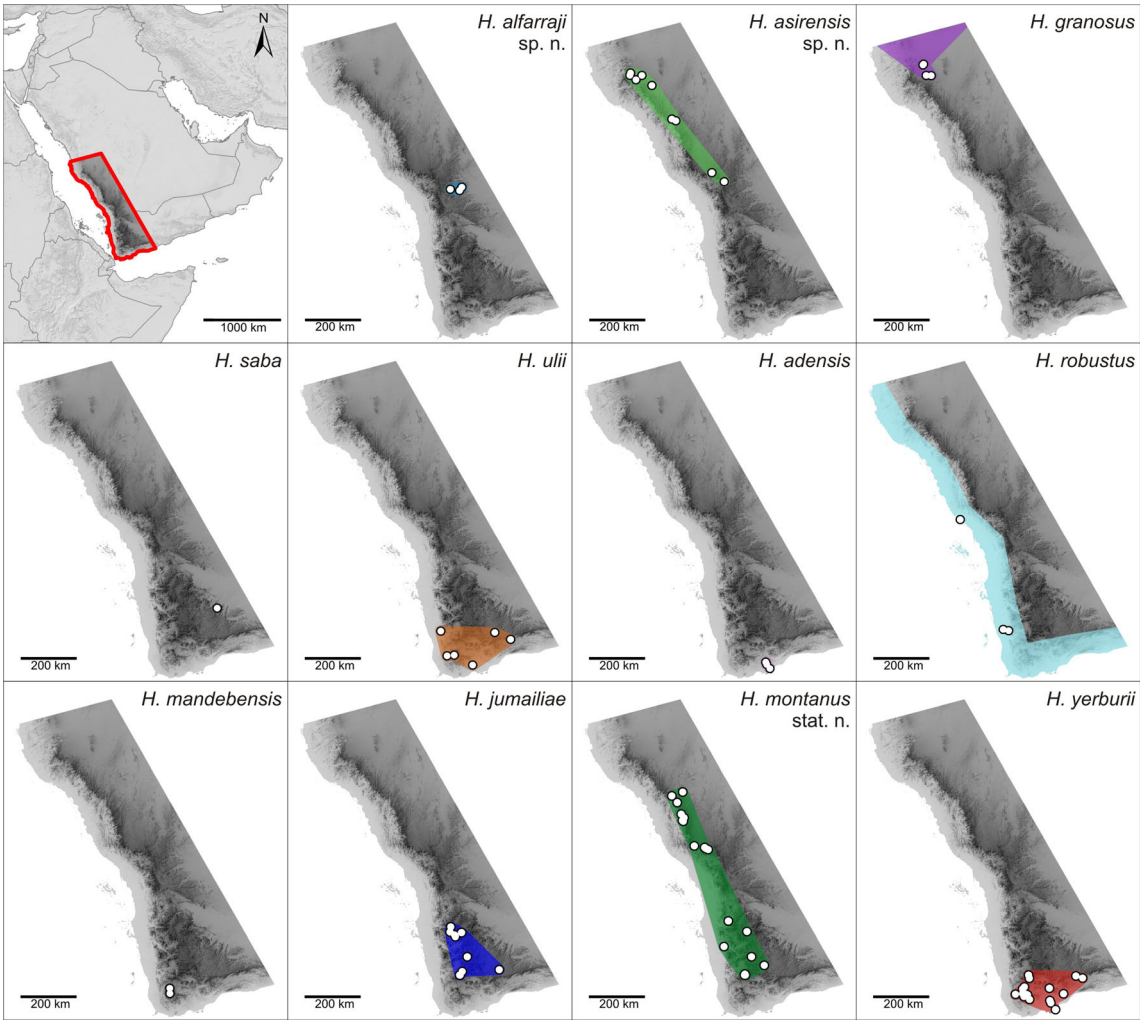

Fig. 3 Sampling sites and distributional ranges estimated by the Convex Hull function with an additional 10-km buffer of all SW Arabian Arid clade *Hemidactylus* species. For detailed information on the localities, GPS coordinates, altitude, GenBank accessions, and voucher codes of all specimens, see Table S2. The range of *H. granosus* was estimated based on all localities reported for the species, i.e., even those located outside the range of this study; the range of *H. robustus* was drawn by hand as a 50–100-km-wide belt along the coast based on known distribution of the species

was not supported by the BF test. Based on all these results, we conclude that *H. y. pauciporosus* is a full species, *Hemidactylus pauciporosus* Lanza, 1978. It should be noted that the only specimen of *H. pauciporosus* available for genetic analyses to date (CAS 227511) was in previous publications (Carranza and Arnold 2012; Gómez-Díaz et al. 2012; Šmíd et al. 2013a) misidentified as *H. macropholis* and that the true *H. macropholis* appeared for the first time in Garcia-Porta et al. (2016). The absence of support of the speciation between *H. pauciporosus* and *H. granchii* under the assumption of large ancestral population sizes is further discussed below.

The status of *H. y. montanus* is also reassessed. It was reconstructed as sister to *H. y. yerburii* in the *BEAST analysis performed here as well as in all analyses of concatenated data performed elsewhere (Busais and Joger 2011b; Šmíd et al. 2013a; Garcia-Porta et al. 2016). Although the two taxa share some alleles in three out of the four studied loci (Fig. 2b), their split that was dated to occur 1.7 Ma (HPD 1.0–2.5) was well supported under all tested scenarios (BPP pp = 1.0 in all cases; Fig. 2a). They furthermore differ significantly in their altitudinal distribution and head shape (Figs. 4, S2). All these multiple lines of evidence strongly support the elevation of *H. y. montanus* to full species status, *Hemidactylus montanus* Busais and Joger, 2011.

The two isolated lineages obtained in the ML analysis within the *saba* group (Fig. S1) and composed of the new material from Saudi Arabia were confirmed to be closely related to *H. granosus* by the *BEAST analysis. The common ancestors of these three species diverged consecutively 2.8 Ma (HPD 1.8–3.9) and 0.9 Ma (HPD 0.4–1.3). Especially the latter divergence occurred relatively recently, yet the speciation probabilities of both nodes under all tested population size and between-species divergence depth scenarios were strongly

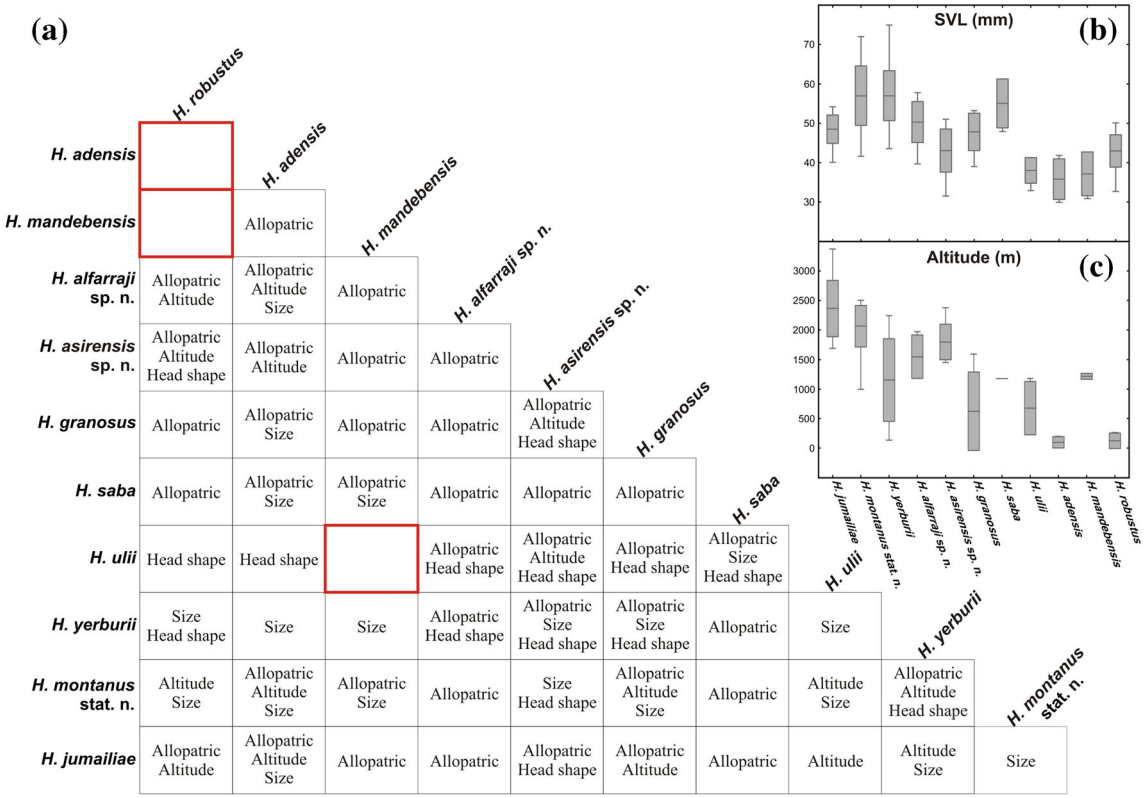

Fig. 4 **a** Pairwise comparisons of the geographical, altitudinal, and morphological overlap of the 11 *Hemidactylus* species occurring in SW Arabia. For each species pair, all criteria in which the two species differ are given. Four differential factors were tested: sympatry/allopatry, difference in preferred altitude, head shape difference, and size difference. Cells outlined in *red* indicate species pairs that do not differ in any of the tested criteria. **b** Comparison of body size (expressed as snout-vent length) of the 11 species. **c** Comparison of the altitudinal distribution of the 11 species. In both **b** and **c**, mean values are shown (*central line*) together with the standard deviation (*box*), and minimum and maximum values (*whiskers*) and species are sorted equally. (Color figure online)

supported (BPP pp = 1.0 in all cases; Fig. 2a). As a result of the molecular differentiation and also the presence of obvious morphological differences, we describe the two new lineages endemic to Saudi Arabia as new species.

Hemidactylus alfarraji sp. n.

Synonymy. Hemidactylus yerburii in: Arnold (1980, 1986); Carranza and Arnold (2006, 2012); Moravec et al. (2011).

Holotype. NMP 75269 (sample code HSA35, Fig. 5), adult male, Saudi Arabia, Najran Province, 32 km W of Najran (17.529° N, 43.827° E, 1969 m a.s.l.), May 24, 2012, collected by S. Carranza, M. Shobrak, and T. Wilms, MorphoBank M390464–M390480.

Paratypes. NMP 75270 (sample code HSA36, MorphoBank M390450–M390463), IBES 10303 (HSA43, MorphoBank M390355–M390366), adult females; IBES 10266 (HSA37, MorphoBank M390434–M390449), IBES 10295 (HSA41, MorphoBank M390379–M390392), adult males; all paratypes have the same collection data as the holotype.

Other material examined. Seven other specimens in total; see Table S2 for details. Juveniles were used for genetic analyses only. Specimens from BMNH were used only for analyses of morphological characters.

Etymology. The species epithet "*alfarraji*" is a genitive Latin noun to honor Dr. Saud Al Farraj for his life-long dedication and contribution to the herpetology of Saudi Arabia, raising public awareness of biodiversity protection and contribution to education at all school levels.

Diagnosis. A species of the Arabian radiation of the Arid clade of *Hemidactylus* characterized by (1) medium size with a maximum recorded SVL 57.8 mm (48.7–57.8 in males, 45.4–52.6 in females); (2) long, wide, and robust head clearly distinct from the neck, particularly in males (HL = 24–29 % of SVL; HW = 10.3 ± 0.4 mm st. dev. in males, 9.1 ± 0.9 mm in females); (3) uppermost nasals always separated by a small median scale; (4) large anterior postmentals in wide mutual contact and in contact with the first and second infralabial; (5) 7–9 infralabials and 8–11 supralabials; (6) dorsum with 14–16 longitudinal rows of enlarged, strongly keeled, conical tubercles; (7) males with invariably 4 preanal pores; (8) 7–8 lamellae under the first toe and 10–12 lamellae under the fourth toe; (9) enlarged tile-like subcaudals; and (10) brownish-beige coloration with distinct dark bands starting behind nostrils and crossing the eyes to the ear openings, dorsum with slightly

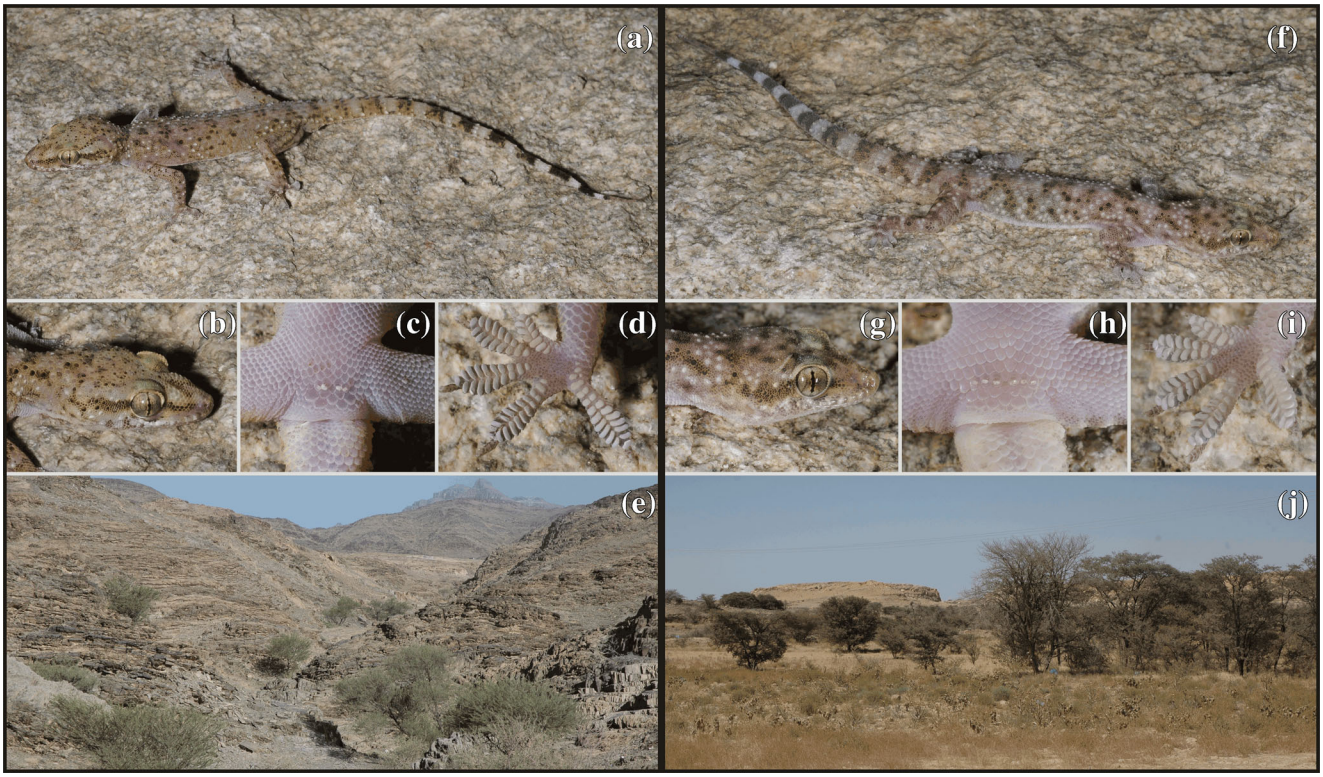

Fig. 5 Holotypes and type localities of *H. alfarraji* sp. n. and *H. asirensis* sp. n. **a** General body habitus of *H. alfarraji* sp. n. holotype (NMP 75269); **b** detail of its head; **c** detail of its precloacal region with preanal pores visible; **d** lamellae under the toes of left hind limb; **e** type locality 32 km W of Najran (1969 m a.s.l.), Najran Province, Saudi Arabia. **f** General body habitus of *H. asirensis* sp. n. holotype (NMP 75271); **g** detail of its head; **h** detail of the precloacal region with preanal pores visible; **i** lamellae under the toes of left hind limb; **j** type locality Al Balhy (2376 m a.s.l.), Asir Province, Saudi Arabia

visible X-shaped dark markings (most distinct in juveniles) formed by dark tubercles, and intact tail with 10–11 intensely dark bands on a beige background, becoming paler towards the tail tip so the dark bands are most contrasting at the end of the tail.

Differential diagnosis. Hemidactylus alfarraji sp. n. is not significantly different in body size and head shape from its closest relatives, *H. granosus* and the new species endemic to the Asir Mountains described below, although it is seemingly the biggest of the three species (Fig. 4). It is significantly distinct from these species by the following characters: the number of infralabials in *H. alfarraji* sp. n. (8.5 ± 0.5, range 7–9) is higher than in *H. granosus* (7.4 ± 0.4, 7–8) and the new species endemic to the Asir Mountains (7.7 ± 0.5, 7–9) (one-way ANOVA $F_{(2,\ 47)} = 17.849$, $p < 0.001$). The number of supralabials is also higher in *H. alfarraji* sp. n. (10.2 ± 0.6, 9–11) than in *H. granosus* (9.3 ± 0.5, 9–11) and the new species endemic to the Asir Mountains (9.4 ± 0.7, 7–11) (one-way ANOVA $F_{(2,\ 47)} = 6.467$, $p < 0.01$). *Hemidactylus alfarraji* sp. n. has a lower number of preanal pores in males (invariably four) than *H. granosus* (5.7 ± 0.8, 4–7) and the new species endemic to the Asir Mountains have (invariably six) (one-way ANOVA $F_{(2,\ 17)} = 24.663$, $p < 0.001$). From the new species endemic to the Asir Mountains, it further differs in having distinctly keeled dorsal tubercles and a higher number of subdigital lamellae under the first toe (7.1 ± 0.3, 7–8 in *H. alfarraji* sp. n. vs. 6.2 ± 0.4, 5–7 in the latter; *t* test $t = 6.247$, $p < 0.001$; Fig. 5). Although the above described significant differences between the species support their species status, the high overlap of scale counts indicates that these characters are of limited use in species identification. Comparison of metric and meristic variables with the other SW Arabian *Hemidactylus* is given in Table S4.

Description of the holotype. NMP 75269 (sample code HSA35), adult male with distinctly depressed body. The head is flattened and very wide in the temporal region. There are enlarged distinctly keeled dorsal tubercles arranged in 14 longitudinal rows along the body. Large eyes protrude from the lateral head outline (in life). Round nostrils are defined by a large rostral with a pronounced median notch, three subequal nasals, and the first labial. The uppermost nasals are not in contact; they are separated by a small inserted pentagonal scale. The supralabials are 10 (left)/11 (right), the infralabials 8/8. The anterior postmentals are in a wide median contact and in contact with the first and second infralabials and are followed by paired posterior postmentals on each side. The ear opening is oval. The head is dorsally covered with regularly spaced round unkeeled tubercles that start at the interorbital level and

continue onto the neck and body where they form keeled tubercles. The ventrals are roughly hexagonal and imbricate. The limbs are slender. The forearms, thighs, and lower legs have large unkeeled tubercles that are pointed caudally. The lamellae on the underside of toes are well developed and distinctly extended towards the toe tips. The lamellae under the first toe are 7/7, under the fourth toe 11/11. Thumbs are very short. The tail is complete, longer than SVL (TL/SVL = 1.27) and with 12 whorls bearing at least six tubercles. Tail whorls are separated by three to five rows of small scales. The subcaudals are enlarged and start about 1 cm behind the vent. There are four preanal pores in a slightly curved line separated medially by one ventral scale. The tongue was removed for genetic analyses.

Measurements (in mm): SVL 52.7, TL 66.8, HL 13.3, HW 10.1, HD 4.1, E 3.2, AG 21.6.

Coloration in life. Background is pale grey-buff to beige; a dark stripe runs from the nostril through the eye to the temporal region and widens distinctly above the ear. There is a dark V-shaped marking on top of the nasal region. The enlarged tubercles on the head are dark. There is a series of dark and almost round vertebral spots that encompass only two vertebral rows of tubercles and the smaller scales between them. The spots start on the nape, the first four (up to scapulae) are most distinct, and those from the scapular region to the vent are less prominent. Some tubercles on flanks, forearms, thighs, and lower legs are also dark. The ventral side is creamy white to pinkish. The tail has 11 dark bands that get darker and more clearly bordered towards the tail tip. They do not extend onto the ventral side of the tail except for the three most posterior bands.

*Morphological variation***.** Original morphometric and meristic data are provided in Table S2. All specimens are very similar regarding size, body proportions, and coloration. Adult male SVL varies from 48.7 to 57.8 mm, in females from 45.4 to 52.6 mm. Paratype IBES 10266 is the only specimen with seven infralabials (unilaterally). Likewise, paratype IBES 10295 is the only specimen with eight supralabials (unilaterally). All examined animals have anterior postmentals in contact with first and second infralabials except BMNH 1992.173, in which anterior postmentals touch only the first infralabial, being separated from the second infralabial by a small interstitial granule. Dorsal tubercles form 16 rows in IBES 10278 and IBES 10302 and 15 in IBES 10303, otherwise always 14. BMNH 1992.172 is the only specimen with 8 lamellae under the first toe and 12 under the fourth toe.

All specimens generally agree in coloration. The dark dorsal tubercles of the juveniles (IBES 10278, IBES 10288) form three clear X-shaped markings, one on scapulae, one in middorsum, and one just in front of the pelvic area.

*Genetic variation***.** The level of genetic variability within *H. alfarraji* sp. n. is very low, perhaps due to the geographic proximity of both localities from where material for genetic analyses was available. Maximum *p* distance is 1.1 % in the *12S* and 2 % in the *cytb*. Variability in the nuclear genes is also rather low, although all loci studied are represented by more than one allele (Fig. 2b). All *rag2* alleles of *H. alfarraji* sp. n are private, while in the *mc1r* and *rag1* usually the central allele is shared with the other new species described herein and also with *H. saba* in the *cmos*.

*Distribution and ecology***.** This new species is endemic to Saudi Arabia. All known localities lie in the Najran area of Saudi Arabia by the Yemeni border in a radius of ca. 40 km (Fig. 3), although it may be more widespread. All the specimens were found during the day inside drainage tunnels under roads that prevent the roads from flooding during torrential rains. The tunnels were located at tributary gorge at a rocky area with scattered *Acacia tortolis* trees. Otherwise, the vegetation cover comprised *Indigofera spinosa, Aristida pennei*, and *Lycium shawii.* One specimen was found between 9 and 9:30 at locality 17.599° N 44.205° E, 1364 m a.s.l., with the air temperature outside the tunnel 30 °C and relative air humidity 29 %; the rest of the specimens were collected between 10:30 and 10:45 at the type locality with the air temperature outside the tunnel 29.7 °C and relative air humidity 25.3 %. No searches were conducted during the night for security reasons and because a sandstorm hit the area during the only night spent at Najran. Future studies of this Saudi endemic should be directed to obtain more information on its distribution and ecology.

***Hemidactylus asirensis* sp. n.**

Synonymy. Hemidactylus yerburii in: Arnold (1980, 1986); Carranza and Arnold (2012).

*Holotype***.** NMP 75271 (sample code HSA44, Fig. 5), adult male, Saudi Arabia, Asir Province, Al Balhy (18.075° N, 43.083° E, 2376 m a.s.l.), May 24, 2012, collected by S. Carranza, M. Shobrak, and T. Wilms, MorphoBank M389997–M390014.

Paratypes. NMP 75272 (sample code HSA12, MorphoBank M390048–M390066), adult male, Saudi Arabia, Asir Province, 5 km N of Wadi Shora (19.836° N, 41.776° E, 1750 m a.s.l.), May 22, 2012; IBES 10044 (sample code HSA2, MorphoBank M390067–M390077), adult male, Saudi Arabia, Makkah Province, 20 km NE of Al Sir (21.259° N, 40.796° E, 1594 m a.s.l.), May 22, 2012; IBES 10011 (HSA4, MorphoBank M390102–M390120, adult female), IBES 10341 (HSA7, MorphoBank M389944–M389962, adult female), IBES 10386 (HSA8, MorphoBank M389919–M389929, adult female), IBES 10330 (HSA6, MorphoBank M389978–M389995, adult male), Saudi Arabia, Makkah Province, 10 km S of Al Sir (21.115° N, 40.599° E, 1696 m a.s.l.), May 21, 2012; IBES 10221 (sample code HSA52, MorphoBank M390031–M390047), adult female, Saudi Arabia, Makkah Province, 7 km S of Ghazaial (20.928° N,

41.123° E, 1453 m a.s.l.), May 25, 2012; IBES 10378 (sample code HSA53, MorphoBank M389930–M389943), adult female, Saudi Arabia, Makkah Province, Taif (21.338° N, 40.422° E, 1616 m a.s.l.), May 27, 2012. All paratypes have the same collectors as the holotype.

*Other material examined***.** Eighteen other specimens in total; see Table S2 for details. Specimens from BMNH were used only for analyses of morphological characters.

Etymology. The species epithet "*asirensis*" is an adjective which refers to the mountain range where the species is distributed, the Asir Mountains of Saudi Arabia.

Diagnosis. A member of the Arabian radiation of the Arid clade of *Hemidactylus* with the following combination of characters: (1) medium size with SVL ranging between 43.0 and 48.5 mm in males and 38.3 and 51.1 mm in females; (2) long and narrow head not wider than the body in its widest part (HL = 23–28 % of SVL, HW = 7.9 ± 1.3 mm in males, 7.6 ± 1.0 mm in females); (3) large anterior postmentals usually in wide mutual median contact (96 % of specimens) and in contact with the first and second infralabial (at least on one side in 96 % of specimens); (4) uppermost nasals separated by an inserted scale in 87 % of specimens; (5) 7–9 infralabials and 7–11 supralabials; (6) dorsum with enlarged tubercles in 12–16 longitudinal rows, the tubercles are not keeled or, if so, only the vertebral ones; (7) males with 6 preanal pores; (8) 5–7 lamellae under the first toe and 9–11 under the fourth toe; (9) enlarged tile-like subcaudals; (10) beige background coloration with dark blotches in irregular vertebral and paravertebral rows that form X-shaped markings, head with distinct dark band from the nostril through eye to the ear, parietal and temporal regions with irregular dark markings which can be absent in some individuals, tail with 9–12 dark bands that grow in intensity towards the tail tip, and body underside creamy whitish.

Differential diagnosis. Hemidactylus asirensis sp. n. differs significantly from its sister species, *H. granosus*, in the head shape; it has shorter and narrower head (HL 10.7 ± 1.3 vs. 12.3 ± 1.1 mm, *t* test $t = -4.085$, $p < 0.001$; HW 7.8 ± 1.2 vs. 9.3 ± 0.8 mm, *t* test $t = -4.407$, $p < 0.001$; Fig. S2) and in the degree of keeling of the dorsal tubercles (*H. asirensis* sp. n. has flat unkeeled tubercles while *H. granosus* strongly keeled). The two species also differ in the number of lamellae under toes; *H. asirensis* sp. n. has 6.2 ± 0.4 (range 5–7) lamellae on the first toe while *H. granosus* has 7.4 ± 0.5 (7–8) (*t* test $t = -8.681$, $p < 0.001$) and 10.1 ± 0.6 (9–11) on the fourth toe while *H. granosus* has 11.6 ± 0.7 (10–13) (*t* test $t = -7.051$, $p < 0.001$). The differences from *H. alfarraji* sp. n. are described above. A comparison of metric and meristic variables with the other *Hemidactylus* species form SW Arabia is given in Table S4.

Description of the holotype. NMP 75271 (sample code HSA44), adult male with a slender body habitus. The head is long (HL = 24 % of SVL) and narrow (HW = 8.5 mm). There are enlarged round dorsal tubercles arranged in 14 longitudinal rows along the body. Round nostrils are defined by a large rostral, three subequal nasals, and the first labial. The uppermost nasals are not in contact. The supralabials are 9/8, the infralabials 8/8. The anterior postmentals are very long and in a wide median contact and in contact with only the first postmentals. The ear opening is kidney-shaped. The head is dorsally covered with small granules intermixed with irregularly spaced round unkeeled tubercles that start at the interorbital level and continue onto the neck and body where they transform to dorsal tubercles. The ventrals are imbricate in regular diagonal rows. The forearms, thighs, and lower legs are covered with round enlarged unkeeled tubercles. The lamellae on the underside of toes are well developed. The lamellae under the first toe are 6/6, under the fourth toe 9/10. The tail is original but broken in the middle and almost detached from the rest of the body; it is longer than the body (TL/SVL = 1.22) and has 11 whorls bearing at least six tubercles. The tail whorls are separated by four to five rows of small scales. The subcaudals are enlarged, tile-like, and wider than long. There are six preanal pores in almost straight line separated medially by one inserted ventral scale. The tongue was removed for genetic analyses.

Measurements (in mm): SVL 45.2, TL 55.2, HL 10.9, HW 8.5, HD 3.8, E 2.5, AG 18.4.

Coloration in life. Background color is beige-brownish; a dark stripe runs from the nostril through the eye to the temporal region. The top of head has several isolated and almost round dark brown spots. There are five clearly visible X-shaped markings on the dorsum, first on the nape, second in the scapular region, two on midbody, last on the sacral region. The markings continue onto the tail in a form of nine dark transverse bands that get darker and more clearly bordered towards the tail tip. The last 7 mm of the tail are brown. The last four dark tail bands are visible also from the underside. The tubercles on the dorsum and flanks that do not form the X-shaped marks are clearly whitish. The venter is uniformly creamy pinkish.

*Morphological variation***.** Original morphometric and meristic data for all examined specimens are in Table S2. All examined specimens have seven to eight infralabials with the exception of the paratypes IBES 10221 and IBES 10386 that both have unilaterally nine infralabials. Paratype IBES 10044 is the only specimen with only 7 (unilaterally) supralabials; all other specimens have 8–11. In BMNH 1978.905, anterior postmentals are not in contact with each other. In IBES 10378, IBES 10011, and BMNH 1934.10.20.8, uppermost nasals are not separated by an inserted scale and are in narrow (IBES 10378) or broad (IBES 10011, BMNH 1934.10.20.8) contact. Number of lamellae under first toe varies from six to seven in most specimens but BMNH 1978.907, in which there are only five (unilaterally) lamellae. The holotype differs from all other examined specimens in

that it is the only individual with anterior postmentals in contact with only the first and not the second infralabials.

Color pattern is consistent among all specimens with only the dark dorsal markings varying in intensity. In some individuals (IBES 10341, IBES 10386), the dark X-shaped dorsal markings are fragmented and formed only by isolated dark blotches.

Genetic variation. There is a certain degree of intraspecific genetic variation in the mtDNA genes in *H. asirensis* sp. n. (Fig. S1) with maximum *p* distance being 3.9 % in the *12S* and 5.6 % in the *cytb*. Consistently with the mtDNA variation, the four nuclear loci also show some genetic structure. Although there are some private alleles of *H. asirensis* sp. n. not shared with any other species, there is allele sharing with some other species in all the nuclear loci analyzed. Some *mc1r* and *cmos* alleles are shared with *H. granosus* and *H. alfarraji* sp. n., *cmos* also with *H. saba*. The central and most frequent alleles are shared with *H. alfarraji* sp. n. in the *rag1* and with *H. granosus* and even with *H. robustus*, *H. mandebensis*, and *H. adensis* in the *rag2*.

Distribution and ecology. This species is endemic to Saudi Arabia. All nine localities from which *H. asirensis* sp. n. is reported here are situated in high altitude areas of the Asir Mountains in Saudi Arabia with elevations ranging from 1453 to 2376 m. They all lie on the eastern foothills of the mountain slopes that face the inland Arabian deserts (Fig. 3), and although it is an arid environment, temperature conditions are much milder than in the surrounding lowland areas. The specimens were collected while active at night (18:30–20:30) and during the day (15:00–15:20) hiding inside drainage tunnels under roads that prevent the roads from flooding during torrential rains. Temperatures on the collection site ranged between 27.5 and 32.1 °C and the relative air humidity between 16.1 and 55.5 %. Most of the tunnels were found in wadis with sandy/gravel substrate in otherwise rocky areas. The vegetation cover was dominated by *Acacia gerrardii* and *A. asak* in the northern sites and *A. tortolis* in the southern sites. Other dominant plant species were *Arstida* sp., *Forsskaolea tenacissima*, *Tamarix aphylla*, and *Juniperus procera*. This gecko species was widely collected between 1934 and 1935 around and inside Taif city by St John Philby and later on, in 1978, by John Gasperetti.

Discussion

The mountains of the SW Arabian Peninsula are well known for their pronounced species richness and high endemism of reptiles (e.g., Arnold 1987; Gasperetti 1988), yet the mechanisms responsible for such diversity have never been investigated. It can be attributed in part to the relative scarcity of data from this region in combination with incomplete taxonomic classification of many groups and the lack of robust phylogenetic knowledge that would form a backbone for such studies. *Hemidactylus* is an exception in that it is presently the best studied Arabian reptile genus with well resolved taxonomy and reliably reconstructed biogeographic history (Busais and Joger 2011a, b; Moravec et al. 2011; Carranza and Arnold 2012; Gómez-Díaz et al. 2012; Šmíd et al. 2013a, b, 2015; Vasconcelos and Carranza 2014). More detailed analyses of the diversification processes underlying its Arabian radiation were therefore feasible.

The species tree analysis of the *saba*, *robustus*, and *yerburii* groups performed here and based on five loci (mtDNA and four nDNA) supports the topology retrieved earlier from the analyses of concatenated data sets (Šmíd et al. 2013a). The only exception is the position of *H. awashensis*, which is sister to all other species of the *robustus* group according to the species tree analysis, a result concordant with previous studies (Šmíd et al. 2015; Garcia-Porta et al. 2016). It is worth noting that we performed the coalescent-based species tree estimation because the method is generally superior to concatenation, which can be prone to producing different tree resolution (Kubatko and Degnan 2007). This is so particularly for trees with short branching intervals or with conflicting gene trees (Degnan and Rosenberg 2009; Lambert et al. 2015), as is the case in the Arabian *Hemidactylus* (Šmíd et al. 2015). The biggest difference between the species tree produced here compared to the previous study, which was based on concatenation and employed the same calibration approach based on mutation rates (Šmíd et al. 2013a), was the divergence dates. Employing the multigene coalescent-based approach resulted in a general pattern of more recent divergence times for all nodes. To be exact, the basal split within the *yerburii* group occurred 6.6 Ma (HPD 5.4–7.9) compared to 9.8 Ma (HPD 6.5–13.6) in the concatenated analysis, the basal split in the *robustus* group 4.2 Ma (HPD 3.3–5.1) compared to 7.0 Ma (HPD 4.6–9.8), and in the *saba* group 5.6 Ma (HPD 4.6–6.6) compared to 7.0 Ma (HPD 4.3–10.0). The split between *H. y. yerburii* and *H. y. montanus* as dated here took place 1.7 Ma (HPD 1.0–2.5) compared to 4.0 Ma (HPD 2.5–5.7). The split of *H. granosus* from *H. asirensis* sp. n. occurred relatively recently, 0.9 Ma (HPD 0.4–1.3). These two separated from *H. alfarraji* sp. n. 2.8 Ma (HPD 1.8–3.9). Despite being based on the same rates for the same genes and implemented with the same priors (Carranza and Arnold 2012), the dating estimates differed slightly with a general pattern of more recent mean divergence times for all nodes in the species tree analysis, although the HPD intervals of the two approaches show a large degree of overlap. The mean difference of dating estimates between the species-tree and gene-tree analyses across all nodes is 2.5 Ma. This is most likely a result of the fact that gene divergences do not necessarily have to correspond to the actual timing of speciation events, but their divergence may be older than the speciation, and that phylogenies derived from concatenated data sets for that reason overestimate divergence

times (Edwards and Beerli 2000; McCormack et al. 2011). Moreover, the presence of shared alleles in all four nDNA genes studied (Fig. 2b) indicates that incomplete lineage sorting is widespread among Arabian *Hemidactylus*. Closely related yet morphologically different species share alleles at most of the studied loci. Only the African *H. awashensis* in the *robustus* group has all alleles of all loci private. The presence of incomplete lineage sorting together with the relatively recent speciation of some of the clades suggest that some of the species are in a stage of incipient speciation (e.g., *H. granosus* and *H. asirensis* sp. n.) and that they have not yet attained reciprocal monophyly in individual genes.

The taxonomy of the Arabian *Hemidactylus* is very advanced compared to other Arabian reptile genera (e.g., Metallinou et al. 2015), although their superficial morphological similarity may cast doubts on the validity of the taxa. Nonetheless, the speciation probabilities estimated by the BPP analyses under all combinations of ancestral population sizes and divergence depths among species together with a careful assessment of some informative morphological characters, such as the preanal pores and the lamellae under the toes (among others), unequivocally support that speciation has occurred in all the nodes of the species tree and that all the recently described species are not a result of taxonomy artificially inflated by species oversplitting (Zachos 2015). Speciation was supported even for the most recent split between *H. granosus* and *H. asirensis* sp. n. that occurred only 0.9 Ma (HPD 0.4–1.3) (Fig. 2a). The low support of speciation for the split between *H. granchii* and *H. pauciporosus* received under the assumption of a large ancestral population size prior was most likely caused by having only a single sample (two alleles of phased nDNA loci) of each available for the analyses. Since large populations assume larger allelic variation, having low sample size with low variation of alleles violates this assumption and results in low support for the speciation event. The two species diverged relatively long ago according to our dating results (3.3 Ma with HPD 2.1–4.5 or 4.7 Ma with HPD 2.7–7.0 according to the alternative dating; Šmíd et al. 2013a). We presume that adding more specimens of the two species rather than sequencing more loci might help to support the speciation, a practice generally recommended for multilocus coalescent-based approaches (Hovmöller et al. 2013). Alternatively, the low BPP support in this node could result from incomplete lineage sorting (see above) and thus the lack of information in the sequence data (Zhang et al. 2014). However, because *H. granchii* and *H. pauciporosus* share alleles only in the *cmos* (Fig. 2b), we assume the former explanation to be more plausible.

The results of the geographical and altitudinal overlap analyses and body size and head shape comparisons clearly show that either geographical differentiation, morphological niche partitioning, or the combination of both has accompanied the speciation history in SW Arabian *Hemidactylus*. Allopatry is the most common diversification mechanism. Of the 55 pairwise between-species comparisons, 40 (73 % species pairs) do not overlap geographically (Figs. 3 and 4), and in the cases when two species differ in one attribute only, allopatry is the most frequent (68 %; 15 of 22 comparisons). Interestingly, altitude alone is responsible for differentiation of only one species pair—*H. jumailiae* and *H. ulii*. Given the complex topography of SW Arabia, with the sharp escarpment rising abruptly from almost sea level up to 2500 m (Fig. 1), one would expect that altitude plays a more substantial role in the ecological separation of species. Apparently, not the high mountains themselves but rather the landscape complexity and habitat heterogeneity are the most likely factors responsible for the numerous allopatric speciation events. It can be assumed that when most of the *Hemidactylus* species are separated geographically, an altitudinal shift is not needed. Our analyses indicate that sympatry is usually accompanied by either body size or head shape differences. These morphological prerequisites are in accord with the character displacement hypothesis (Brown and Wilson 1956) and have been considered a prerequisite necessary for the coexistence of closely related lizard species (Pianka 1986 and references therein). In *Hemidactylus*, extreme body size disparities caused by accelerated rates of body size evolution, but not coupled with head shape differentiation, have been confirmed for sympatric species of the Socotra Archipelago (Garcia-Porta et al. 2016). Also, in the mainland species studied here, body size disparities were found more frequently (36 %; 20 of 55 comparisons) than is head shape differentiation (27 %; 15 of 55 comparisons). For instance, *H. yerburii* differs from the five other species with which it occurs in sympatry by being larger than the others and *H. ulii* separates from *H. robustus* and *H. adensis*, with which it is sympatric, solely by head shape (Fig. 4). Head shape has been indicated to be a good predictor of bite performance in lizards (Herrel et al. 2001), and it is usually correlated with specialization for different prey sizes (Metzger and Herrel 2005). It is therefore possible that *H. ulii* feeds on different prey items than do *H. robustus* and *H. adensis*. This however requires further study.

Interestingly, there are three species pairs that do not show significant differences in any of the tested criteria—*H. robustus* and *H. adensis*, *H. robustus* and *H. mandebensis*, and *H. ulii* and *H. mandebensis* (Fig. 4). *Hemidactylus robustus*, *H. adensis*, and *H. mandebensis* are closely related species that have diverged relatively recently, 2.8 Ma (HPD 1.9–3.7). *Hemidactylus robustus* is a widespread species with an extensive range (see Sindaco and Jeremčenko 2008). It is assumed to have originated in eastern Arabia (Oman) as revealed by its high genetic diversity in this region (Carranza and Arnold 2012; Šmíd et al. 2013a); elsewhere, its distribution is limited to coastal areas. A likely explanation of its morphological similarity and geographical overlap with *H. adensis* and *H. mandebensis* is that

H. robustus has been introduced to SW Arabia relatively recently by human-mediated dispersal and its ecological separation from the other species has not developed yet. Another case is the *H. ulii–H. mandebensis* species pair. Both species originated in the southwestern corner of the Arabian Peninsula, and their ranges are most likely not a result of human-mediated translocations. Yet, they do not show any significant geographic or morphological differences in any of the characters studied (Fig. 4). Nevertheless, even seemingly sympatric and phenotypically similar species can co-occur if they have different microhabitat requirements (Pianka 1969; Vitt and de Carvalho 1995) and *H. ulii* and *H. mandebensis* can separate out just by microhabitat selection. Unfortunately, the data currently available do not allow for testing such fine-scale ecological divergence.

According to the results of the dating analyses presented here, the intra-Arabian diversification began 6.2 Ma (HPD 5.2–7.3; Fig. 2a) when the *robustus* and *saba* groups separated and were followed by the separation of *H. ulii*, which split off 5.6 Ma (HPD 4.6–6.6). Although the divergence estimates for these two splits were dated as older in the analyses of concatenated data (9.5 Ma with HPD 6.4–13.3 and 7.0 Ma with HPD 4.3–10.0, respectively; Šmíd et al. 2013a), the HPD intervals of the latter were much larger and always overlapped with those of the current analyses. For instance, the HPD interval of the split of *H. ulii* based on concatenation encompasses entirely that of the species tree approach. However, even after taking this uncertainty associated with divergence dating into account, we can still draw tentative conclusions on the diversification history of *Hemidactylus* in SW Arabia. The onset and subsequent rise of the number of speciation events appears to be linked with gradual climatic changes that occurred in Arabia during the Miocene–Pliocene boundary. The climate of Arabia was extremely dry during the Late Miocene (~10–5.5 Ma), and the conditions had changed dramatically to humid in the Early Pliocene (Edgell 2006; Huang et al. 2007). Throughout the Pliocene, savannah grasslands and woodlands dominated the area until aridity began to increase again towards the end of the Pliocene and resulted in hyper arid conditions similar to today in most of the Arabian mainland (Edgell 2006). The results of the dating analyses show that the onset of *Hemidactylus* diversification could be coincident with the establishment of the SW Arabia monsoon system 8–4.6 Ma and that most of the speciation events took place during the humid climatic phase between 5.5 and 0.8 Ma (Fig. 2a). Moreover, SW Arabia is also the area of mainland Arabia that receives the highest annual precipitation (Edgell 2006). It therefore seems that despite the species of the *Hemidactylus* Arid clade generally inhabit extremely arid environments, temporal and spatial precipitation increase has been the key factor that triggered its speciation and sustained its diversity in the Arabian Peninsula. Whether and to what degree the precipitation-related factors influenced the species distributions during the Quaternary climatic oscillations remains to be tested with approaches such as paleo-distribution modeling which requires more distributional data than we have currently available (1–19 unique localities).

By elevating the two former *H. yerburii* subspecies to species ranks, one more species (*H. montanus*) becomes endemic to SW Arabia and one (*H. pauciporosus*) to the Horn of Africa. Together with the two new species described herein, this further supports SW Arabia as one of the world's richest reptile hotspots. Additionally, detailed phylogenetic analyses of other Arabian reptile genera that shed light on the biogeographic history and potential species richness of some widespread taxa have been produced in recent years (Metallinou et al. 2012, 2015; Kapli et al. 2014; de Pous et al. 2016; Tamar et al. 2016). They give good grounds for expecting that the overall reptile diversity of southern Arabia will increase once their taxonomy is sorted out. This highlights the singularity of the Eastern Afromontane and Horn of Africa biodiversity hotspots that extend onto the southwestern part of the Arabian Peninsula and which represent the richest non-tropical reptile hotspots (Mittermeier et al. 2004).

Acknowledgements We would like to thank all curators who granted us access to or provided tissue samples of material housed in their collections, namely, B. Clarke, E. N. Arnold, and P. D. Campbell (BMNH); J. Vindum (CAS); R. Sindaco, and G. Boano (MCCI); G. Doria (MSNG); S. Scali (MSNM); A. Nistri (MZUF); J. Moravec (NMP); S. B. El Din (SMB); G. Köhler, and L. Acker (SMF). Special thanks are due to T. Mazuch (TMHC) for providing pictures of the syntype of *H. yerburii*. We are thankful to the Deanship of academic research at the Taif University for funding and issuing collection permit for sampling in Saudi Arabia (Grant No. 1–433–2108). We thank Omer Baeshen, Environment Protection Agency, Sana'a, Republic of Yemen, for issuing the collection permit (Ref 10/2007). The manuscript benefitted from comments of two anonymous reviewers, and the English was significantly improved by Jessica da Silva and Jody Taft. This work was supported by the Ministry of Culture of the Czech Republic under grant DKRVO 2016/15, National Museum, 00023272 (JŠ), and grant CGL2015-70390-P (MINECO-FEDER) (SC).

References

Arnold, E. N. (1980). The reptiles and amphibians of Dhofar, southern Arabia. *Journal of Oman Studies, Special Report, 2*, 273–332.

Arnold, E. N. (1986). A key and annotated check-list to the lizards and amphisbaenians of Arabia. *Fauna of Saudi Arabia, 8*, 385–435.

Arnold, E. N. (1987). Zoogeography of the reptiles and amphibians of Arabia. In F. Krupp, W. Schneider, & R. Kinzelbach (Eds.), *Proceedings of the Symposium on the fauna and zoogeography of the Middle East* (pp. 245–256). Wiesbaden: Ludwig Reichert.

Baele, G., Lemey, P., Bedford, T., Rambaut, A., Suchard, M. A., & Alekseyenko, A. V. (2012). Improving the accuracy of demographic and molecular clock model comparison while accommodating phylogenetic uncertainty. *Molecular Biology and Evolution, 29*(9), 2157–2167.

Baele, G., Li, W. L. S., Drummond, A. J., Suchard, M. A., & Lemey, P. (2013). Accurate model selection of relaxed molecular clocks in

Bayesian phylogenetics. *Molecular Biology and Evolution, 30*(2), 239–243.

Bohannon, R. G., Naeser, C. W., Schmidt, D. L., & Zimmermann, R. A. (1989). The timing of uplift, volcanism, and rifting peripheral to the Red Sea: a case for passive rifting? *Journal of Geophysical Research, 94*(B2), 1683–1701.

Böhme, M., & Ilg, A. (2003). *FosFARbase*. http://www.wahre-staerke.com/. Accessed April 18, 2016.

Bosworth, W., Huchon, P., & McClay, K. (2005). The Red Sea and Gulf of Aden Basins. *Journal of African Earth Sciences, 43*(1–3), 334–378.

Brown, W. L., & Wilson, E. O. (1956). Character displacement. *Systematic Zoology, 5*(2), 49–64.

Burbrink, F. T., & Guiher, T. J. (2015). Considering gene flow when using coalescent methods to delimit lineages of North American pitvipers of the genus *Agkistrodon*. *Zoological Journal of the Linnean Society, 173*(2), 505–526.

Busais, S., & Joger, U. (2011a). Molecular phylogeny of the gecko genus *Hemidactylus* Oken, 1817 on the mainland of Yemen (Reptilia: Gekkonidae). *Zoology in the Middle East, 53*, 25–34.

Busais, S., & Joger, U. (2011b). Three new species of *Hemidactylus* Oken, 1817 from Yemen (Squamata, Gekkonidae). *Vertebrate Zoology, 61*(2), 267–280.

Camargo, A., Morando, M., Avila, L. J., & Sites, J. W. (2012). Species delimitation with ABC and other coalescent-based methods: a test of accuracy with simulations and an empirical example with lizards of the *Liolaemus darwinii* complex (Squamata: Liolaemidae). *Evolution, 66*(9), 2834–2849.

Carranza, S., & Arnold, E. N. (2006). Systematics, biogeography and evolution of *Hemidactylus* geckos (Reptilia: Gekkonidae) elucidated using mitochondrial DNA sequences. *Molecular Phylogenetics and Evolution, 38*, 531–545.

Carranza, S., & Arnold, E. N. (2012). A review of the geckos of the genus *Hemidactylus* (Squamata: Gekkonidae) from Oman based on morphology, mitochondrial and nuclear data, with descriptions of eight new species. *Zootaxa, 3378*, 1–95.

Castresana, J. (2000). Selection of conserved blocks from multiple alignments for their use in phylogenetic analysis. *Molecular Biology and Evolution, 17*(4), 540–552.

Clement, M., Posada, D., & Crandall, K. A. (2000). TCS: A computer program to estimate gene genealogies. *Molecular Ecology, 9*(10), 1657–1659.

Cox, N., Mallon, D., Bowles, P., Els, J., & Tognelli, M. (2012). The conservation status and distribution of reptiles of the Arabian Peninsula. by: IUCN, Gland, Switzerland and Cambridge, UK and the Environment and Protected Areas Authority.

Darriba, D., Taboada, G. L., Doallo, R., & Posada, D. (2012). JModelTest 2: more models, new heuristics and parallel computing. *Nature Methods, 9*(8), 772.

Davison, I., Al-Kadasi, M., Al-Khirbash, S., Al-Subbary, A. K., Baker, J., Blakey, S., et al. (1994). Geological evolution of the southeastern Red Sea Rift margin, Republic of Yemen. *Geological Society of America Bulletin, 106*(11), 1474–1493.

de Pous, P., Machado, L., Metallinou, M., Červenka, J., Kratochvíl, L., Paschou, N., et al. (2016). Taxonomy and biogeography of *Bunopus spatalurus* (Reptilia; Gekkonidae) from the Arabian Peninsula. *Journal of Zoological Systematics and Evolutionary Research, 54*(1), 67–81.

Degnan, J. H., & Rosenberg, N. A. (2009). Gene tree discordance, phylogenetic inference and the multispecies coalescent. *Trends in Ecology & Evolution, 24*(6), 332–340.

dos Santos, A. M., Cabezas, M. P., Tavares, A. I., Xavier, R., Branco, M. (2015). tcsBU: a tool to extend TCS network layout and visualization. *Bioinformatics 32*(4), 627–628. doi:10.1093/bioinformatics/btv636.

Drummond, A. J., & Bouckaert, R. R. (2015). *Bayesian evolutionary analysis with BEAST*. New York: Cambridge University Press.

Drummond, A. J., Suchard, M. A., Xie, D., & Rambaut, A. (2012). Bayesian phylogenetics with BEAUti and the BEAST 1.7. *Molecular Biology and Evolution, 29*(8), 1969–1973.

Edgell, H. S. (2006). *Arabian deserts: nature, origin and evolution*. Dordrecht: Springer.

Edwards, S., & Beerli, P. (2000). Perspective: gene divergence, population divergence, and the variance in coalescence time in phylogeographic studies. *Evolution, 54*(6), 1839–1854.

Estes, R. (1983). *Handbuch der Paläoherpetologie; Part 10A: Sauria terrestria, Amphisbaenia*. Stuttgart, New York: Gustav Fischer Verlag.

Fjeldså, J., & Rahbek, C. (2006). Diversification of tanagers, a species rich bird group, from lowlands to montane regions of South America. *Integrative and Comparative Biology, 46*(1), 72–81.

Fjeldså, J., Bowie, R. C., & Rahbek, C. (2012). The role of mountain ranges in the diversification of birds. *Annual Review of Ecology, Evolution, and Systematics, 43*, 249–265.

Flot, J. F. (2010). Seqphase: a web tool for interconverting phase input/output files and fasta sequence alignments. *Molecular Ecology Resources, 10*(1), 162–166.

Frontier, S. (1976). Étude de la décroissance des valeurs propres dans une analyse en composantes principales: Comparaison avec le moddle du bâton brisé. *Journal of Experimental Marine Biology and Ecology, 25*(1), 67–75.

Garcia-Porta, J., Šmíd, J., Sol, D., Fasola, M., & Carranza, S. (2016). Testing the island effect on phenotypic diversification: insights from the *Hemidactylus* geckos of the Socotra Archipelago. *Scientific Reports, 6*, 23729.

Gasperetti, J. (1988). Snakes of Arabia. *Fauna of Saudi Arabia, 9*, 169–450.

Gómez-Díaz, E., Sindaco, R., Pupin, F., Fasola, M., & Carranza, S. (2012). Origin and in situ diversification in *Hemidactylus* geckos of the Socotra Archipelago. *Molecular Ecology, 21*(16), 4074–4092.

Grummer, J. A., Bryson, R. W., & Reeder, T. W. (2014). Species delimitation using Bayes factors: simulations and application to the *Sceloporus scalaris* species group (Squamata: Phrynosomatidae). *Systematic Biology, 63*(2), 119–133.

Heled, J., & Drummond, A. J. (2010). Bayesian inference of species trees from multilocus data. *Molecular Biology and Evolution, 27*(3), 570–580.

Herrel, A., Damme, R. V., Vanhooydonck, B., & Vree, F. D. (2001). The implications of bite performance for diet in two species of lacertid lizards. *Canadian Journal of Zoology, 79*(4), 662–670.

Hovmöller, R., Knowles, L. L., & Kubatko, L. S. (2013). Effects of missing data on species tree estimation under the coalescent. *Molecular Phylogenetics and Evolution, 69*(3), 1057–1062.

Huang, Y., Clemens, S. C., Liu, W., Wang, Y., & Prell, W. L. (2007). Large-scale hydrological change drove the late Miocene C4 plant expansion in the Himalayan foreland and Arabian Peninsula. *Geology, 35*(6), 531–534.

Joly, S., Stevens, M. I., & van Vuuren, B. J. (2007). Haplotype networks can be misleading in the presence of missing data. *Systematic Biology, 56*(5), 857–862.

Kapli, P., Lymberakis, P., Crochet, P. A., Geniez, P., Brito, J. C., Almutairi, M., et al. (2014). Historical biogeography of the lacertid lizard *Mesalina* in North Africa and the Middle East. *Journal of Biogeography, 42*(2), 267–279.

Kass, R. E., & Raftery, A. E. (1995). Bayes factors. *Journal of the American Statistical Association, 90*(430), 773–795.

Katoh, K., & Standley, D. M. (2013). MAFFT multiple sequence alignment software version 7: improvements in performance and usability. *Molecular Biology and Evolution, 30*(4), 772–780.

Kohler, T., & Maselli, D. (2012). *Mountains and climate change. From understanding to action*. Bern: FAO/CDE/SDC.

Kubatko, L. S., & Degnan, J. H. (2007). Inconsistency of phylogenetic estimates from concatenated data under coalescence. *Systematic Biology, 56*(1), 17–24.

Lambert, S. M., Reeder, T. W., & Wiens, J. J. (2015). When do species-tree and concatenated estimates disagree? An empirical analysis with higher-level scincid lizard phylogeny. *Molecular Phylogenetics and Evolution, 82*, 146–155.

Lanfear, R., Calcott, B., Ho, S. Y. W., & Guindon, S. (2012). PartitionFinder: combined selection of partitioning schemes and substitution models for phylogenetic analyses. *Molecular Biology and Evolution, 29*(6), 1695–1701.

Leaché, A. D., & Fujita, M. K. (2010). Bayesian species delimitation in West African forest geckos (*Hemidactylus fasciatus*). *Proceedings of the Royal Society B: Biological Sciences, 282*(1819), 1–7.

Losos, J. B. (2009). *Lizards in an evolutionary tree: ecology and adaptive radiation of anoles*. Berkeley: University of California Press.

Martin, D. P., Lemey, P., Lott, M., Moulton, V., Posada, D., & Lefeuvre, P. (2010). RDP3: a flexible and fast computer program for analyzing recombination. *Bioinformatics, 26*(19), 2462–2463.

McCormack, J. E., Huang, H., Knowles, L. L., Gillespie, R., & Clague, D. (2009). Sky islands. *Encyclopedia of Islands, 4*, 841–843.

McCormack, J. E., Heled, J., Delaney, K. S., Peterson, A. T., & Knowles, L. L. (2011). Calibrating divergence times on species trees versus gene trees: implications for speciation history of *Aphelocoma* jays. *Evolution, 65*(1), 184–202.

Metallinou, M., Arnold, E. N., Crochet, P.-A., Geniez, P., Brito, J. C., Lymberakis, P., et al. (2012). Conquering the Sahara and Arabian deserts: systematics and biogeography of *Stenodactylus* geckos (Reptilia: Gekkonidae). *BMC Evolutionary Biology, 12*(258), 1–17.

Metallinou, M., Červenka, J., Crochet, P.-A., Kratochvíl, L., Wilms, T., Geniez, P., et al. (2015). Species on the rocks: systematics and biogeography of the rock-dwelling *Ptyodactylus* geckos (Squamata: Phyllodactylidae) in North Africa and Arabia. *Molecular Phylogenetics and Evolution, 85*, 208–220.

Metzger, K. A., & Herrel, A. (2005). Correlations between lizard cranial shape and diet: a quantitative, phylogenetically informed analysis. *Biological Journal of the Linnean Society, 86*(4), 433–466.

Miller, M., Pfeiffer, W., & Schwartz, T (2010). Creating the CIPRES Science Gateway for inference of large phylogenetic trees. In *Proceedings of the Gateway Computing Environments Workshop (GCE)*, (pp. 1–8). New Orleans.

Mittermeier, R. A., Gil, P. R., Hoffmann, M., Pilgrim, J., Brooks, T., Mittermeier, C. G., et al. (2004). *Hotspots Revisited: Earth's Biologically Richest and Most Endangered Terrestrial Ecoregions*. Washington: Conservation International.

Moravec, J., Kratochvíl, L., Amr, Z. S., Jandzik, D., Šmíd, J., & Gvoždík, V. (2011). High genetic differentiation within the *Hemidactylus turcicus* complex (Reptilia: Gekkonidae) in the Levant, with comments on the phylogeny and systematics of the genus. *Zootaxa, 2894*, 21–38.

Myers, N., Mittermeier, R. A., Mittermeier, C. G., da Fonseca, G. A. B., & Kent, J. (2000). Biodiversity hotspots for conservation priorities. *Nature, 403*, 853–858.

Pepper, M., Fujita, M. K., Moritz, C., & Keogh, J. S. (2011). Palaeoclimate change drove diversification among isolated mountain refugia in the Australian arid zone. *Molecular Ecology, 20*(7), 1529–1545.

Pianka, E. R. (1969). Sympatry of desert lizards (*Ctenotus*) in Western Australia. *Ecology, 50*, 1012–1030.

Pianka, E. R. (1986). *Ecology and natural history of desert lizards: analyses of the ecological niche and community structure*. New Jersey: Princeton University Press.

Popp, M., Gizaw, A., Nemomissa, S., Suda, J., & Brochmann, C. (2008). Colonization and diversification in the African 'sky islands' by Eurasian *Lychnis* L. (Caryophyllaceae). *Journal of Biogeography, 35*(6), 1016–1029.

Rambaut, A., & Drummond, A. (2007). Tracer v1.4. Available from: http://beast.bio.ed.ac.uk/Tracer.

Rannala, B., & Yang, Z. (2003). Bayes estimation of species divergence times and ancestral population sizes using DNA sequences from multiple loci. *Genetics, 164*(4), 1645–1656.

Silvestro, D., & Michalak, I. (2012). RaxmlGUI: a graphical front-end for RAxML. *Organisms Diversity and Evolution, 12*(4), 335–337.

Sindaco, R., & Jeremčenko, V. K. (2008). *The reptiles of the Western Palearctic. 1. Annotated checklist and distributional atlas of the turtles, crocodiles, amphisbaenians and lizards of Europe, North Africa, Middle East and Central Asia*. Latina (Italy): Monografie della Societas Herpetologica Italica - I. Edizioni Belvedere.

Sindaco, R., Metallinou, M., Pupin, F., Fasola, M., & Carranza, S. (2012). Forgotten in the ocean: systematics, biogeography and evolution of the *Trachylepis* skinks of the Socotra Archipelago. *Zoologica Scripta, 41*(4), 346–362.

Sindaco, R., Venchi, A., & Grieco, C. (2013). *The reptiles of the Western Palearctic. 2. Annotated checklist and distributional atlas of the snakes of Europe, North Africa, Middle East and Central Asia, with an update to the Vol. 1.*. Latina (Italy): Monografie della Societas Herpetologica Italica - I. Edizioni Belvedere.

Šmíd, J., Mazuch, T., & Sindaco, R. (2014). An additional record of the little known gecko *Hemidactylus granchii* Lanza, 1978 (Reptilia: Gekkonidae) from Somalia. In M. Capula, & C. C. (Eds.), *Scripta Herpetologica. Studies on Amphibians and Reptiles in honour of Benedetto Lanza* (pp. 165–169). Latina (Italy): Societas Herpetologica Italica.

Šmíd, J., Carranza, S., Kratochvíl, L., Gvoždík, V., Nasher, A. K., & Moravec, J. (2013a). Out of Arabia: a complex biogeographic history of multiple vicariance and dispersal events in the gecko genus *Hemidactylus* (Reptilia: Gekkonidae). *PLoS ONE, 8*(5), e64018.

Šmíd, J., Moravec, J., Kratochvíl, L., Gvoždík, V., Nasher, A. K., Busais, S., et al. (2013b). Two newly recognized species of *Hemidactylus* (Squamata, Gekkonidae) from the Arabian Peninsula and Sinai, Egypt. *ZooKeys, 355*, 79–107.

Šmíd, J., Moravec, J., Kratochvíl, L., Nasher, A. K., Mazuch, T., Gvoždík, V., et al. (2015). Multilocus phylogeny and taxonomic revision of the *Hemidactylus robustus* species group (Reptilia, Gekkonidae) with descriptions of three new species from Yemen and Ethiopia. *Systematics and Biodiversity, 13*(4), 346–368.

Stamatakis, A. (2006). RAxML-VI-HPC: maximum likelihood-based phylogenetic analyses with thousands of taxa and mixed models. *Bioinformatics, 22*(21), 2688–2690.

Stephens, M., Smith, N. J., & Donnelly, P. (2001). A new statistical method for haplotype reconstruction from population data. *American Journal of Human Genetics, 68*(4), 978–989.

Talavera, G., & Castresana, J. (2007). Improvement of phylogenies after removing divergent and ambiguously aligned blocks from protein sequence alignments. *Systematic Biology, 56*(4), 564–577.

Tamar, K., Scholz, S., Crochet, P.-A., Geniez, P., Meiri, S., Schmitz, A., et al. (2016). Evolution around the Red Sea: systematics and biogeography of the agamid genus *Pseudotrapelus* (Squamata: Agamidae) from North Africa and Arabia. *Molecular Phylogenetics and Evolution, 97*, 55–68.

Tamura, K., Stecher, G., Peterson, D., Filipski, A., & Kumar, S. (2013). MEGA6: molecular evolutionary genetics analysis version 6.0. *Molecular Biology and Evolution, 30*(12), 2725–2729.

Templeton, A. R., Crandall, K. A., & Sing, C. F. (1992). A cladistic analysis of phenotypic associations with haplotypes inferred from restriction endonuclease mapping and DNA sequence data. III. Cladogram estimation. *Genetics, 132*(2), 619–633.

Vanhooydonck, B., & Van Damme, R. (1999). Evolutionary relationships between body shape and habitat use in lacertid lizards. *Evolutionary Ecology Research, 1*(7), 785–805.

Vasconcelos, R., & Carranza, S. (2014). Systematics and biogeography of *Hemidactylus homoeolepis* Blanford, 1881 (Squamata:

Gekkonidae), with the description of a new species from Arabia. *Zootaxa, 3835*(4), 501–527.

Vitt, L. J., & de Carvalho, C. M. (1995). Niche partitioning in a tropical wet season: lizards in the lavrado area of northern Brazil. *Copeia, 2*, 305–329.

Wollenberg, K. C., Vieites, D. R., Van Der Meijden, A., Glaw, F., Cannatella, D. C., & Vences, M. (2008). Patterns of endemism and species richness in Malagasy cophyline frogs support a key role of mountainous areas for speciation. *Evolution, 62*(8), 1890–1907.

Yang, Z. (2014). BP&P Version 3. Available at http://abacus.gene.ucl.ac.uk/software.html.

Yang, Z., & Rannala, B. (2010). Bayesian species delimitation using multilocus sequence data. *Proceedings of the National Academy of Sciences, 107*(20), 9264–9269.

Zachos, F. E. (2015). Taxonomic inflation, the phylogenetic species concept and lineages in the Tree of Life—a cautionary comment on species splitting. *Journal of Zoological Systematics and Evolutionary Research, 53*(2), 180–184.

Zhang, C., Rannala, B., & Yang, Z. (2014). Bayesian species delimitation can be robust to guide-tree inference errors. *Systematic Biology, 63*(6), 993–1004.